Hindawi Publishing Corporation
Advances in High Energy Physics
Volume 2013, Article ID 503401, 29 pages
http://dx.doi.org/10.1155/2013/503401

Review Article

Prospects for Neutrino Oscillation Physics

Silvia Pascoli[1] and Thomas Schwetz[2]

[1] *IPPP, Department of Physics, Durham University, Durham DH1 3LE, UK*
[2] *Max-Planck-Institut für Kernphysik, Saupfercheckweg 1, 69117 Heidelberg, Germany*

Correspondence should be addressed to Thomas Schwetz; schwetz@mpi-hd.mpg.de

Received 8 August 2012; Accepted 7 November 2012

Academic Editor: Jose Bernabeu

Recently the last unknown lepton mixing angle θ_{13} has been determined to be relatively large, not too far from its previous upper bound. This opens exciting possibilities for upcoming neutrino oscillation experiments towards addressing fundamental questions, among them the type of the neutrino mass hierarchy and the search for CP violation in the lepton sector. In this paper we review the phenomenology of neutrino oscillations, focusing on subleading effects, which will be the key towards these goals. Starting from a discussion of the present determination of three-flavour oscillation parameters, we give an outlook on the potential of near-term oscillation physics as well as on the long-term program towards possible future precision oscillation facilities. We discuss accelerator-driven long-baseline experiments as well as nonaccelerator possibilities from atmospheric and reactor neutrinos.

1. Introduction

Over the last 15 years so huge progress has been made in the study of neutrino oscillations [1–4], and with the recent determination of the last unknown mixing angle θ_{13} [5–9] a clear first-order picture of the three-flavour lepton mixing matrix has emerged. The results of a global fit [10] to world neutrino oscillation data including data presented at the Neutrino2012 conference are summarized in Figure 1 and Table 1 (for alternative global fits see [11, 12], and combinations of the recent data relevant to the θ_{13} determination have been presented in [13, 14]). Global data as of June 2012 disfavours $\theta_{13} = 0$ with a $\Delta\chi^2 \approx 100$ and its value are determined as $\theta_{13} = (8.6^{+0.44}_{-0.46})^\circ$. (An uncertainty about this number at the level of 1σ remains due to a tension between predicted reactor neutrino fluxes and data from reactor experiments with baselines less than 100 m, the so-called reactor anomaly [15].) Establishing such a relatively large value of θ_{13}, comparable to the previous bound [16], opens exciting possibilities for neutrino oscillations. There are fundamental open questions in neutrino physics which can be addressed with neutrino oscillations.

(i) Is there CP violation in the leptonic sector, as in the quark sector? The behaviour under the CP transformation is one of the fundamental properties of particles and a violation of the CP symmetry might be linked to the baryon asymmetry of the universe.

(ii) What is the hierarchy of the neutrino mass spectrum, normal or inverted? This information is important phenomenologically for the interpretation of other neutrino experiments, for instance, neutrinoless double beta decay. Moreover, together with the absolute mass scale, it is one of the key pieces of information on neutrino masses.

(iii) What are the precise values of the neutrino-mixing angles? Do they show an underlying pattern? The answers to these questions are a necessary input in order to solve the flavour problem.

With our current knowledge of θ_{13} answering those questions becomes a realistic possibility.

The outline of this work is as follows. In Section 2 we review the current status of neutrino oscillations and discuss the phenomenology of long-baseline (LBL), reactor, and atmospheric neutrino experiments. In Section 3 we discuss the potential of currently operating LBL and reactor facilities in the time frame of about 10 years. In Section 4 some nonaccelerator-based methods to determine the neutrino mass hierarchy are discussed. In Section 5 we give an overview on possible long-term experimental strategies

Table 1: Three-flavour oscillation parameters from a fit to global data after the Neutrino2012 conference [10]. The normalization of reactor neutrino fluxes is determined by short-baseline reactor data, which are included in the fit.

	bfp $\pm 1\sigma$	3σ range
$\sin^2\theta_{12}$	0.30 ± 0.013	$0.27 \to 0.34$
$\theta_{12}/^\circ$	33.3 ± 0.8	$31 \to 36$
$\sin^2\theta_{23}$	$0.41^{+0.037}_{-0.025} \oplus 0.59^{+0.021}_{-0.022}$	$0.34 \to 0.67$
$\theta_{23}/^\circ$	$40.0^{+2.1}_{-1.5} \oplus 50.4^{+1.2}_{-1.3}$	$36 \to 55$
$\sin^2\theta_{13}$	0.023 ± 0.0023	$0.016 \to 0.030$
$\theta_{13}/^\circ$	$8.6^{+0.44}_{-0.46}$	$7.2 \to 9.5$
$\delta/^\circ$	300^{+66}_{-138}	$0 \to 360$
$\Delta m^2_{21}/10^{-5}\,\mathrm{eV}^2$	7.50 ± 0.185	$7.00 \to 8.09$
$\Delta m^2_{31}/10^{-3}\,\mathrm{eV}^2$ (NH)	$2.47^{+0.069}_{-0.067}$	$2.27 \to 2.69$
$\Delta m^2_{32}/10^{-3}\,\mathrm{eV}^2$ (IH)	$-2.43^{+0.042}_{-0.065}$	$-2.65 \to -2.24$

towards high-precision oscillation facilities. We do not discuss solar, supernova, or other astrophysical neutrinos which are covered in detail in other chapters of this volume.

We will remain within the three-neutrino mixing framework and will not discuss deviations from it such as sterile neutrinos or nonstandard interactions. We use the standard convention for parametrizing the three-flavour lepton-mixing matrix in terms of the three angles, θ_{12}, θ_{23}, θ_{13}, and one Dirac-type CP phase δ [17]:

$$U = \begin{pmatrix} c_{12}c_{13} & s_{12}c_{13} & s_{13}e^{-i\delta} \\ -s_{12}c_{23} - c_{12}s_{13}s_{23}e^{i\delta} & +c_{12}c_{23} - s_{12}s_{13}s_{23}e^{i\delta} & c_{13}s_{23} \\ +s_{12}s_{23} - c_{12}s_{13}c_{23}e^{i\delta} & -c_{12}s_{23} - s_{12}s_{13}c_{23}e^{i\delta} & c_{13}c_{23} \end{pmatrix}, \tag{1}$$

where $c_{ij} \equiv \cos\theta_{ij}$ and $s_{ij} \equiv \sin\theta_{ij}$. Squared differences of the neutrino masses m_i are defined as $\Delta m^2_{ij} \equiv m^2_i - m^2_j$. The neutrino mass hierarchy is determined by the sign of Δm^2_{31}, with $\Delta m^2_{31} > 0$ corresponding to normal hierarchy (NH), and $\Delta m^2_{31} < 0$ to inverted hierarchy (IH).

2. Present Status as Case Study for Oscillation Phenomenology

In this section we introduce the oscillation probabilities relevant to long-baseline accelerator experiments, reactor experiments, as well as atmospheric neutrinos. We use the present data to illustrate the interplay and complementarity of different types of oscillation experiments.

2.1. The Beam-Reactor Interplay. Since the advent of data on $\nu_\mu \to \nu_e$ searches from T2K [5] and MINOS [6] on the one side, and θ_{13} reactor experiments Double Chooz [7], Daya Bay [8], and RENO [9] on the other side, the long anticipated complementarity of beam and reactor experiments [18, 19] is now a reality. In this section we discuss some aspects of that related to deviations of θ_{23} from maximal mixing, as well as the dependence of the global fit on the CP phase δ.

Recent data seem to indicate a deviation of θ_{23} from the maximal mixing value of 45°, roughly at the level of $1.7\sigma - 2\sigma$, compare Figure 1 (in [12] a somewhat higher significance is obtained). If confirmed, such a deviation would have profound implications for neutrino mass models based on flavour symmetries. An important contribution to this effect comes from recent MINOS data on ν_μ disappearance. Neglecting effects of Δm^2_{21} and the matter effect, the relevant survival probability is given by

$$P_{\nu_\mu \to \nu_\mu} = 1 - 4\left|U_{\mu 3}\right|^2 \left(1 - \left|U_{\mu 3}\right|^2\right) \sin^2 \frac{\Delta m^2_{31} L}{4E}, \qquad \left|U_{\mu 3}\right|^2 = \sin^2\theta_{23}\cos^2\theta_{13}, \tag{2}$$

where L is the baseline and E is the neutrino energy. Hence, the probability is symmetric under $|U_{\mu 3}|^2 \to (1 - |U_{\mu 3}|^2)$. In the two-flavour limit of $\theta_{13} = 0$ this implies that the data is sensitive only to $\sin^2 2\theta_{23}$, which for $\theta_{23} \neq 45^\circ$ leads to a degeneracy between the first and second octants of θ_{23} [20]. Indeed, recent data from MINOS [21] have given a best fit point of $\sin^2 2\theta \approx 0.94$ if analysed in a two-flavour framework.

Since θ_{13} is large, one can try to explore a synergy between long-baseline appearance experiments and an independent determination of θ_{13} at reactor experiments in order to resolve the degeneracy [18, 20, 22]. Let us look at the appearance probability relevant to the $\nu_\mu \to \nu_e$ searches at T2K [5] and MINOS [6]. Expanding to second order in the small parameters $\sin\theta_{13}$ and $\alpha \equiv \Delta m^2_{21}/\Delta m^2_{31}$ and assuming a constant matter density that one finds [23–25]:

$$\begin{aligned} P_{\nu_\mu \to \nu_e} \approx\ & 4\, \sin^2\theta_{13}\, \sin^2\theta_{23} \frac{\sin^2\Delta\,(1-A)}{(1-A)^2} \\ & + \alpha^2 \sin^2 2\theta_{12} \cos^2\theta_{23} \frac{\sin^2 A\Delta}{A^2} \\ & + 2\alpha \sin\theta_{13} \sin 2\theta_{12} \sin 2\theta_{23} \\ & \times \cos\left(\Delta \pm \delta_{\mathrm{CP}}\right) \frac{\sin\Delta A}{A} \ \frac{\sin\Delta\,(1-A)}{1-A}, \end{aligned} \tag{3}$$

with the definitions

$$\Delta \equiv \frac{\Delta m^2_{31} L}{4E}, \qquad A \equiv \frac{2EV}{\Delta m^2_{31}}, \tag{4}$$

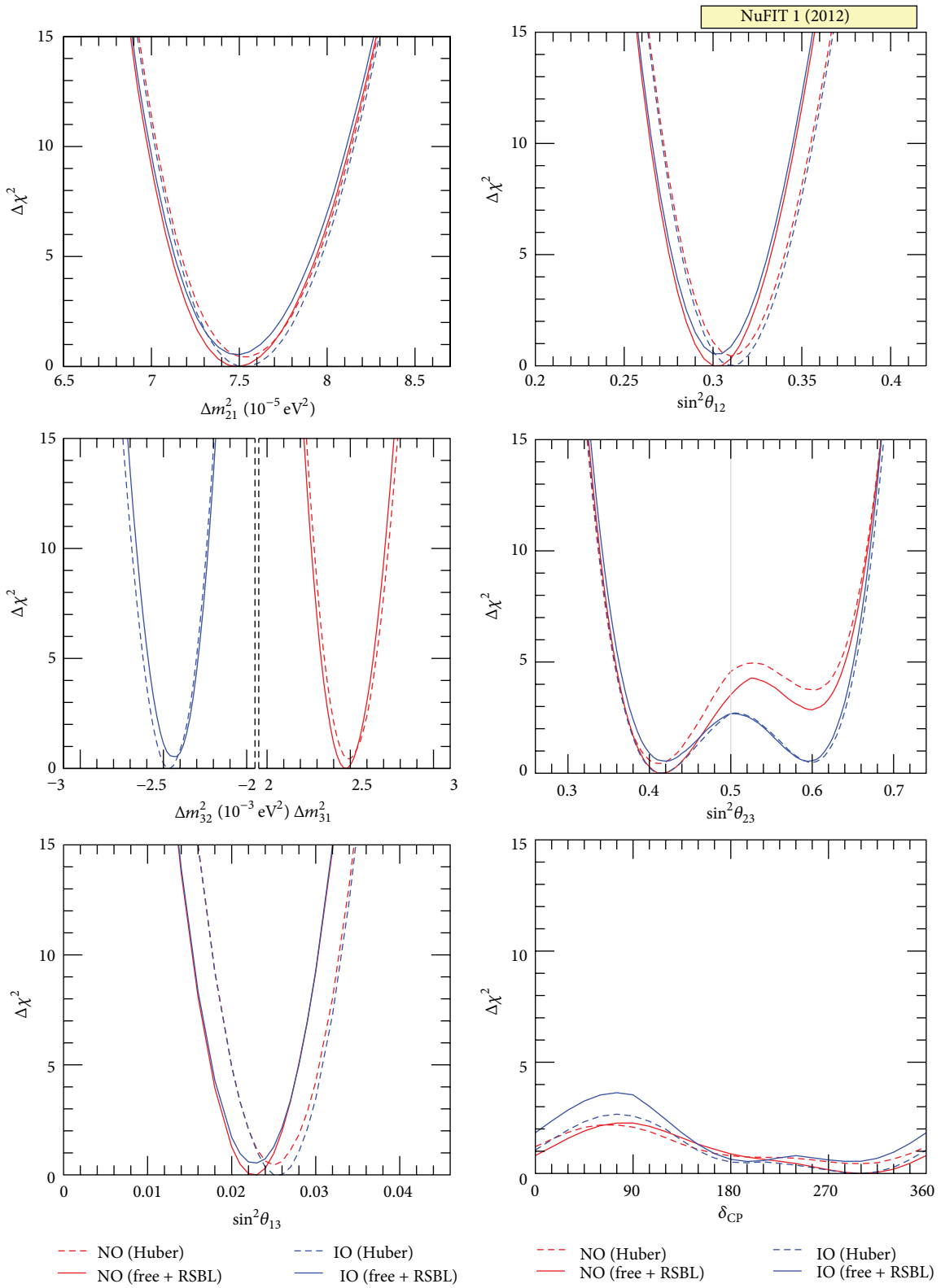

FIGURE 1: Determination of three-flavour oscillation parameters [10]. The red (blue) curves are for NH (IH). Results for different assumptions concerning the analysis of data from reactor experiments are shown: for solid curves the normalization of reactor fluxes is left free, and data from short-baseline (less than 100 m) reactor experiments are included. For dashed curves short-baseline data are not included but reactor fluxes as predicted in [152] are assumed.

where L is the baseline, E is the neutrino energy, and V is the effective matter potential [26]. Note that α, Δ, and A are sensitive to the sign of Δm^2_{31} (i.e., the type of the neutrino mass ordering). The plus (minus) sign in (3) applies for neutrinos (antineutrinos), and for antineutrinos $V \to -V$, which implies that $A \to -A$. It is clear from (3) that in the case of large matter effect, $A \gtrsim 1$, the terms $(1 - A)$ depend strongly on the type of the mass hierarchy, and for $A = 1$ (possible for neutrinos and NH, or antineutrinos and IH) a resonance is encountered [27]. Numerically one finds for a typical matter density of 3 g/cm^3

$$|A| \simeq 0.09 \left(\frac{E}{\text{GeV}}\right) \left(\frac{\left|\Delta m^2_{31}\right|}{2.5 \times 10^{-3}\,\text{eV}^2}\right)^{-1}. \tag{5}$$

Since, for T2K $E \sim 0.7$ GeV, matter effects are of order few percent, whereas in experiments like NOvA [28] with $E \sim 2$ GeV we can have $|A| \sim 0.2$. Note that $\alpha^2 \approx 10^{-3}$, which implies that the second term in the first line of (3) gives a very small contribution compared to the other terms.

An important observation is that the first term in (3) (which dominates for large θ_{13}) depends on $\sin^2\theta_{23}$ and therefore is sensitive to the octant. Reactor experiments with $L \sim 1$ km, on the other hand, provide a measurement of θ_{13} independent of θ_{23}. The relevant survival probability is given by

$$P_{\nu_e \to \nu_e} = 1 - \sin^2 2\theta_{13} \sin^2\Delta + \mathcal{O}\left(\alpha^2\right). \tag{6}$$

Hence, by combining the data from reactor experiments such as Double Chooz [7], Daya Bay [8], and RENO [9] with the appearance data from T2K and MINOS one should be sensitive in principle to the octant of θ_{23}. The situation from present data is illustrated in Figure 2, where we show the determination of θ_{13} from the beam experiments T2K and MINOS as a function of the CP phase δ and the octant of θ_{23}, where we have chosen values motivated by the MINOS disappearance result. The resulting regions in $\sin^2 2\theta_{13}$ are compared to the reactor measurments from DoubleChooz, DayaBay, and RENO. It is clear from that figure that for present data from beams and reactors it is not possible to distinguish between 1st and 2nd θ_{23} octants. For both possibilities overlap regions between beams and reactors can be found although they are at different values of δ. Therefore, current data from reactor and long-baseline beam experiments are not able to resolve the θ_{23} octant degeneracy. The lifting of the degeneracy (at low CL) visible in Figure 1 appears due to atmospheric neutrino data, to be discussed below.

In principle the reactor-beam combination should also offer some sensitivity to the CP phase δ. This is shown in the right panels of Figure 2. We see that if the octant of θ_{23} and the neutrino mass hierarchy were known, already present data from the beam and reactor experiments used in that figure would show quite sizeable dependence on the CP phase, depending on which of the 4 degenerate solutions is considered. However, it is also clear from the figure that we marginalize over those four solutions, $\chi^2(\delta)$ becomes very flat, and essentially all values of δ would be consistent within $\Delta\chi^2 \lesssim 1$. This is a real-life example of how degeneracies can seriously spoil the sensitivity of long-baseline data [29]. The somewhat larger δ dependence visible in Figure 1 follows again from the global fit including atmospheric neutrinos, as discussed below.

2.2. Subleading Effects in Atmospheric Neutrino Oscillations. Atmospheric neutrinos provide a powerful tool to study neutrino oscillations, which is manifest also by the first evidence for oscillations from Super-Kamiokande in 1998 [1]. In this section we briefly discuss subleading oscillation modes, triggered by Δm^2_{21} and/or θ_{13}, and comment on using them for addressing some of the open questions in oscillation physics.

An important property of atmospheric neutrinos is the fact that the neutrino source contains ν_e and ν_μ as well as neutrinos and antineutrinos. Therefore, the contributions to e-like and μ-like event samples can be written schematically as

$$\begin{aligned} N_e &\propto \left(\Phi_e P_{\nu_e \to \nu_e} + \Phi_\mu P_{\nu_\mu \to \nu_e}\right)\sigma_e \\ &= \Phi_e \left(P_{\nu_e \to \nu_e} + r P_{\nu_\mu \to \nu_e}\right)\sigma_e \\ N_\mu &\propto \left(\Phi_e P_{\nu_e \to \nu_\mu} + \Phi_\mu P_{\nu_\mu \to \nu_\mu}\right)\sigma_\mu \\ &= \Phi_\mu \left(\frac{1}{r} P_{\nu_e \to \nu_\mu} + P_{\nu_\mu \to \nu_\mu}\right)\sigma_\mu, \end{aligned} \tag{7}$$

where Φ_α and σ_α are initial flux and detection cross section for neutrino of flavour α, and we have defined the flux ratio

$$r \equiv \frac{\Phi_\mu}{\Phi_e}, \tag{8}$$

with $r \approx 2$ in the sub-GeV range and $r \approx 2.6$–4.5 in the multi-GeV range. In (7) we have suppressed energy and zenith angle dependence, as well as detector resolutions and efficiencies. If the detector cannot identify the charge of the lepton, a sum over neutrino and antineutrinos is implicitly assumed; otherwise, analogous relations hold for neutrinos and antineutrinos separately. Hence, the observation of e-like and μ-like events contains convoluted information on different oscillation channels.

An interesting observable is the excess of e-like events (relative to the no-oscillation prediction N_e^0), since in the two-flavour limit one expects $N_e = N_e^0$, and therefore any deviation of the observed number of events from N_e^0 should be due to subleading effects. The excess can be written in the following way; see, for example, [30]:

$$\begin{aligned} \frac{N_e}{N_e^0} - 1 \approx\ & \left(r \sin^2\theta_{23} - 1\right) P_{2\nu}\left(\Delta m^2_{31}, \theta_{13}\right) \\ & + \left(r \cos^2\theta_{23} - 1\right) P_{2\nu}\left(\Delta m^2_{21}, \theta_{12}\right) \\ & - \sin\theta_{13} \sin 2\theta_{23}\ r\ \text{Re}\left(A^*_{ee} A_{\mu e}\right). \end{aligned} \tag{9}$$

Here $P_{2\nu}(\Delta m^2, \theta)$ is an effective two-flavour oscillation probability governed by a mass-squared difference Δm^2 and a mixing angle θ, and A_{ee} and $A_{\mu e}$ are elements of a transition amplitude matrix. The three terms appearing in (9) have a

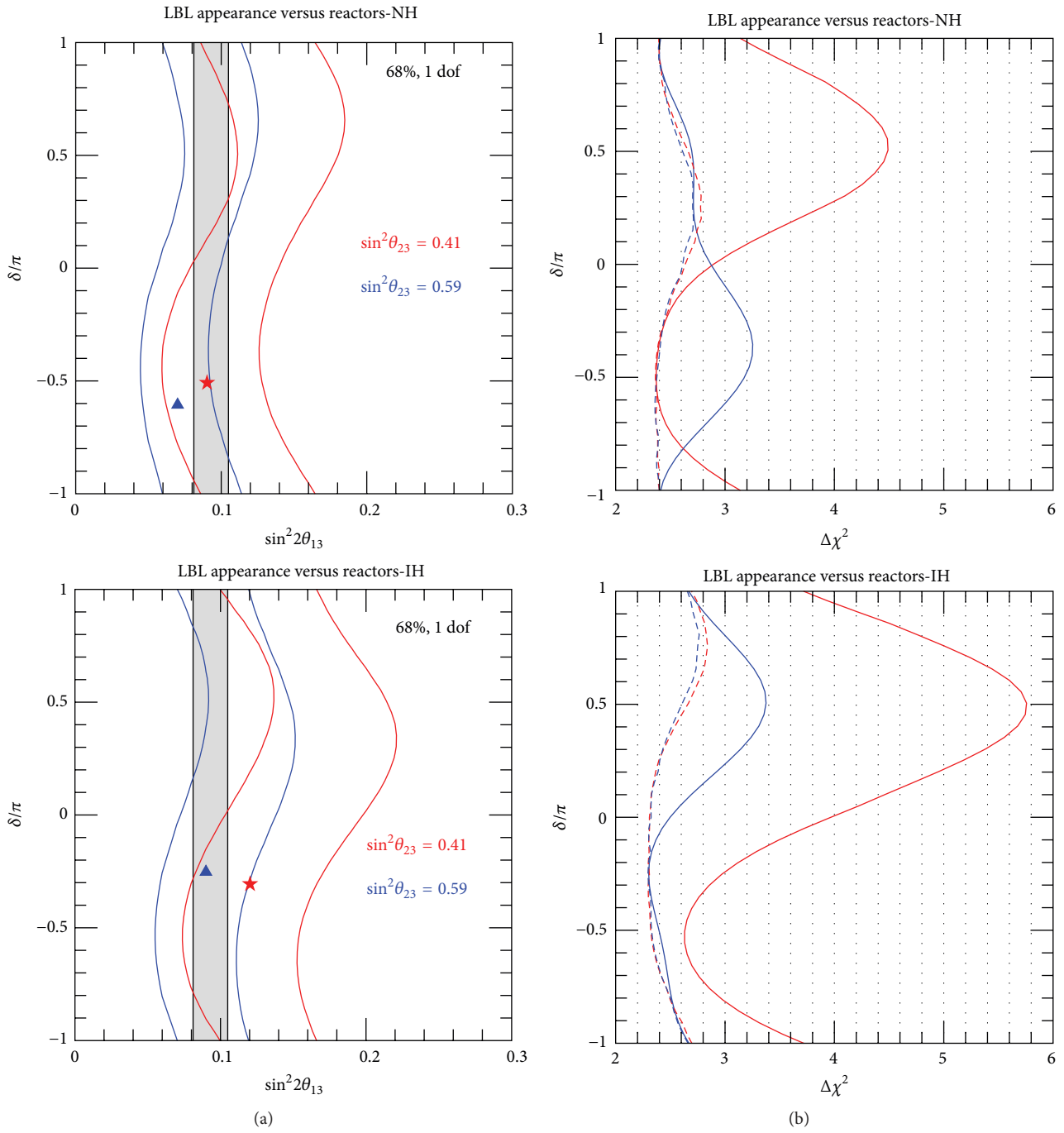

FIGURE 2: (a) Preferred regions in the $\sin^2 2\theta_{13} - \delta$ plane. The contour curves correspond to beams T2K + MINOS, where $\sin^2\theta_{23}$ is fixed to the two degenerate solutions in the 1st (red) and 2nd (blue) octant. The gray region corresponds to the θ_{13} determination from the reactors Double Chooz, Daya Bay, and RENO. (b) $\Delta\chi^2(\delta)$ for beams (dashed) and beams+reactors (solid) with the same color coding as in the left panels. Upper (lower) panels are for NH (IH).

well-defined physical interpretation. The first term is important in the multi-GeV range and is controlled by the mixing angle θ_{13} in $P_{2\nu}(\Delta m^2_{31}, \theta_{13})$. This probability can be strongly affected by resonant matter effects [31–36]. Depending on the mass hierarchy the resonance will occur either for neutrinos or antineutrinos. The second term is important for sub-GeV events, and it takes into account the effect of "solar oscillations" due to Δm^2_{21} and θ_{12} [37–40]. Via the prefactor containing the flux ratio r, both the first and second terms in (9) depend on the octant of θ_{23} though, in oposite directions, the multi-GeV (sub-GeV) excess is suppressed (enhanced) for $\theta_{23} < 45^\circ$. Finally, the last term in (9) is an interference term between θ_{13} and Δm^2_{21} amplitudes, and this term shows also dependence on the CP phase δ [30, 40].

Three neutrino effects may also show up in μ-like events. This is especially interesting for experiments which can only observe muons, such as: for example, the INO or IceCube experiments. For these types of experiments the multi-GeV region is most interesting, where effects Δm^2_{21} are very small. Hence, we can approximate $\Delta m^2_{21} \approx 0$, and following [41, 42] one can write the excess in μ-like events as

$$\frac{N_\mu}{N^0_\mu} - 1 \approx \sin^2\theta_{23}\left(\frac{1}{r} - \sin^2\theta_{23}\right) P_{2\nu}\left(\Delta m^2_{31}, \theta_{13}\right) - \frac{1}{2}\sin^2 2\theta_{23}\left[1 - \mathrm{Re}\left(A_{33}\right)\right]. \quad (10)$$

The first term is controlled by θ_{13} and is subject to resonant matter effects, similar to the first term in (9), though with a different dependence on θ_{23} and the flux ratio. In the second term, A_{33} is a probability amplitude satisfying $P_{2\nu}(\Delta m^2_{31}, \theta_{13}) = 1 - |A_{33}|^2$. In the limit $\theta_{13} = 0$ we have $\mathrm{Re}(A_{33}) = \cos(\Delta m^2_{31} L/2E)$, such that the second term in (10) just describes two-flavour $\nu_\mu \to \nu_\mu$ vacuum oscillations.

2.3. Interplay of Complementary Data Sets in the Present Global Fit. As mentioned above, while MINOS ν_μ disappearance data prefers a nonmaximal value of θ_{23}, we do not observe any sensitivity to the octant of θ_{23} from global data without atmospheric neutrinos. In the global analysis of [10] including atmospheric data a weak preference for the 1st octant is obtained in the case of NH; see Figure 1. Similar results are obtained also in [12] with even somewhat higher significance. This can be attributed to a zenith-angle-independent event excess in the sub-GeV e-like data in SuperKamiokande. Such an excess can be explained by oscillations due to Δm^2_{21} [37–39]. For sub-GeV events the second term in (9) is relevant. In that energy regime $r \approx 2$ and for $\sin^2\theta_{23} \approx 0.5$ the prefactor $(r\cos^2\theta_{23} - 1)$ is suppressed, whereas in the 1st octant with $\sin^2\theta_{23} < 0.5$ an excess is induced. Let us mention that in an official SuperKamiokande analysis [43] this effect is not clearly observed although one should take into account that there is no combined analysis with MINOS data performed. It can be seen from (9) and (10) that there can be some features in e-like or μ-like data samples which exhibit a different dependence on θ_{23}, and which of those subtle effects dominates depends on details of the detector simulation, binning, and treatment of systematic uncertainties. Apparently competing effects become somewhat more important for IH, as in that case the preference for the 1st octant disappears; see Figure 1.

We emphasize the importance of resolving the θ_{23} octant degeneracy in order to obtain sensitivity to the CP phase δ. This can be seen from Figure 2. By favouring one of the two solution for $\sin^2\theta_{23}$ the beam-reactor combination provides a better sensitivity to δ, visible in the right panels. With current data this effect is still small, given the final sensitivity to δ shown in Figure 1, which is at level of $\Delta\chi^2 \approx 3$. We emphasize again the crucial interplay of different data sets necessary for this sensitivity to emerge: MINOS ν_μ disappearance prefers $\sin^2 2\theta_{23} < 1$, atmospheric data slightly disfavours $\sin^2\theta_{23} > 0.5$, and the $\nu_\mu \to \nu_e$ data from beams combined with the θ_{13} determination from reactors provide sensitivity to δ.

3. The Current Generation of Long-Baseline Beam and Reactor Experiments

The reactor experiments, Double Chooz [7], DayaBay [8], and RENO [9], have obtained spectacular results already after few weeks of data taking. All of them are still statistics dominated, and the precision of the determination of θ_{13} will improve considerably for higher exposures. According to the results of [44] (based on assumptions on systematics from the proposals of the three experiments) the ultimate precision will be dominated by DayaBay. Also T2K [5] is essentially only in the "startup phase" (which unfortunately has been interrupted by the 2011 earthquake in Japan). In addition the NOvA experiment [28] will come online soon and will provide additional data on $\nu_\mu \to \nu_e$ appearance. In [45] the expected combined potential of those experiments with their final exposures has been investigated in respect to address the mass hierarchy or a determination of the CP phase δ. Here we review the results obtained there in the light of the by now known value of θ_{13}. The "nominal" exposures are summarized in Table 2. The experimental configurations are based on official documents as of 2009. As a rough rule of thumb those data might be available around 2020.

Let us first discuss the prospects for the θ_{23} measurment, including the determination of the octant in case of a nonmaximal value. Figure 3 shows the ability of T2K + NOvA + DayaBay to reconstruct $\sin^2\theta_{23}$ as a function of its true value. Data on ν_μ disappearance from T2K and NOvA are mainly sensitive to $\sin^2 2\theta_{23}$ (see discussion related to (2)), whereas the combination of the $\nu_\mu \to \nu_e$ appearance data with the θ_{13} reactor measurment provides sensitivity to the octant [18, 20, 22], as discussed above see also Figure 2. While this mechanism does not work for current data, it can be used to identify the right octant at 3σ with projected exposures if $|\sin^2\theta_{23} - 0.5| > 0.1$. Note the slight asymmetry of the regions, which is a consequence of the relatively large value of θ_{13} and can be understood from (2). We also observe that for large deviations from maximality the accuracy on $\sin^2\theta_{23}$ will be quite good, around ± 0.02 at 3σ, whereas close to maximality the determination will be much worse, with a 3σ range of about $0.45 < \sin^2\theta_{23} < 0.58$, due to the flatness of $\sin^2 2\theta$ at $\theta = 45^\circ$.

As we have seen above, already with present data a global fit of all experiments shows a slight dependence on the CP phase δ. On the other hand the mass hierarchy is undistinguishable with a $\Delta\chi^2 \lesssim 1$ between NH and IH, see Figure 1. Now we address the question whether with near-term data from the experiments listed in Table 2 we may be able to say something on the type of the neutrino mass hierarchy or the CP phase δ.

Possible outcome of a global fit to data from the final exposure of T2K, NOvA, and DayaBay is shown in Figure 4. Left (right) panel correspond to NH (IH), and we adopt the two exemplary values of $\delta = \pi/2$ (upper panels) and $3\pi/2$ (lower panels) corresponding to maximal CP violation. The colored regions would be obtained under the assumption of

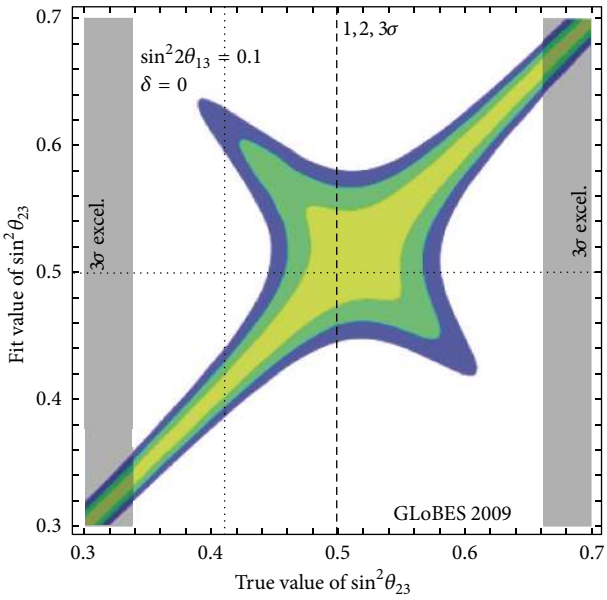

FIGURE 3: Determination of $\sin^2\theta_{23}$ at $1, 2, 3\sigma$ (1 dof) as a function of the true value from T2K, NOvA, and DayaBay with their final exposures according to Table 2. True values of $\sin^2 2\theta_{13} = 0.1$ and $\delta = 0$ have been assumed. The vertical dotted line and the shaded regions indicate the present best fit point and 3σ excluded region, respectively. Figure is based on the results of [45].

known mass hierarchy. In this case some regions of δ can be excluded at 3σ although CP-conserving values 0 or π are always contained in the allowed region, indicating that CP violation cannot be established, even under the assumption of known hierarchy. The detailed study performed in [45] shows that only for less than 30% of all possible values of the phase δ a hint for CP violation at 90% CL may be obtained. Even for upgraded versions of the beams, with increased beam power, extended running time (up to around 2025), and including antineutrino data from T2K CP violation can be "discovered" at 3σ for about 25% of all possible values of δ (see also [46] for related results).

The mass hierarchy determination relies on the matter effect in the $\nu_\mu \rightarrow \nu_e$ transitions. From the experiments considered here only for the NOvA experiment a notable matter effect is present due to the baseline of 812 km. In Figure 4 we illustrate the combined potential to identify the neutrino mass hierarchy. The black contour curves correspond to the allowed regions obtained by fitting the simulated data with the wrong hierarchy. The local χ^2 minimum is marked with a black box and the χ^2 value of the local minimum is given in the figure. It turns out that the four examples shown in the figure correspond approximately to the most optimistic and pessimistic cases for the hierarchy determination. The best possible configuration is obtained for a true NH and $\delta = 3\pi/2$ (left-lower pannel) and a true IH and $\delta = \pi/2$ (right-upper pannel), where the hierarchy can be identified at about 3σ. For the opposite combinations (true NH, $\delta = \pi/2$ and true IH, $\delta = 3\pi/2$) very poor sensitivity is obtained with $\chi^2 \approx 2$. This behaviour can be understood from (3) by considering the sign of the interference term in the second line. Good sensitivity is obtained when, for the channel which is enhanced by the matter resonance (neutrinos for NH or antineutrinos for IH), the CP phase has such a value that the sign of the interference term is positive (constructive interference), which leads to a maximum enhancement of the event numbers in the resonant channel, see also [47].

Unfortunately a significant determination of the mass hierarchy is only possible for very special points in the parameter space, close to the ones shown in Figure 4, lower-left or upper-right panels. Even for a 90% CL hint for the true hierarchy can be obtained only for about 50% of all possible values of δ. With the abovementioned upgrades in beam power and extended running times up to 2025 a 3σ mass hierarchy determination can be reached for about 30–40% of all possible values of δ [45] (see also [48] for a recent analysis).

We conclude that with the upcoming experiments as summarized in Table 2 it will be very hard to address CP violation and the mass hierarchy with reasonable significance, and it seems necessary to consider projects beyond those. Before considering high precision long-baseline facilities designed to address those questions in Section 5 we discuss in the next section alternative ways to determine the neutrino mass hierarchy.

4. Alternative Mass Hierarchy Determinations

The fact that θ_{13} has been found to be relatively large opens interesting possibilities to identify the mass hierarchy, beyond accelerator-driven long-baseline experiments. In this section we mention some of those possibilities, based on θ_{13}-induced matter effects in atmospheric neutrinos as discussed in Section 2.2 by considering different kinds of atmospheric neutrino detectors: magnetized detectors (Section 4.1), huge nonmagnetized detectors using water or liquid argon (Section 4.2), or the IceCube detector (Section 4.3). In Section 4.4 we briefly mention an interesting method based on vacuum oscillations of reactor neutrinos. We do not discuss the possibility to use supernova neutrinos [49–52] or neutrinoless double beta decay [53, 54] to identify the mass hierarchy.

4.1. Atmospheric Neutrinos—Magnetized. The determination of the mass hierarchy based on the matter effect relies on the ability to find out whether the resonant enhancement occurs for neutrinos (which would signal NH) or for antineutrinos (IH). Since atmospheric neutrinos contain both neutrinos and antineutrinos, the sensitivity to the hierarchy (for a given total number of events) is much better if neutrino- and antineutrino-induced events can be distinguished, which can be done if the charge of the charged lepton can be identified. In this respect, magnetized iron calorimeters are a promising technology since they offer excellent charge discrimination for muons with few GeV energies. In particular the ICal experiment at the India-based Neutrino Observatory (INO) [55, 56] aims at the measurment of charge-separated atmospheric neutrino-induced muons. (Sensitivities of a hypothetical magnetized liquid argon detector have been estimated in [57, 58].) In such detectors the identification of

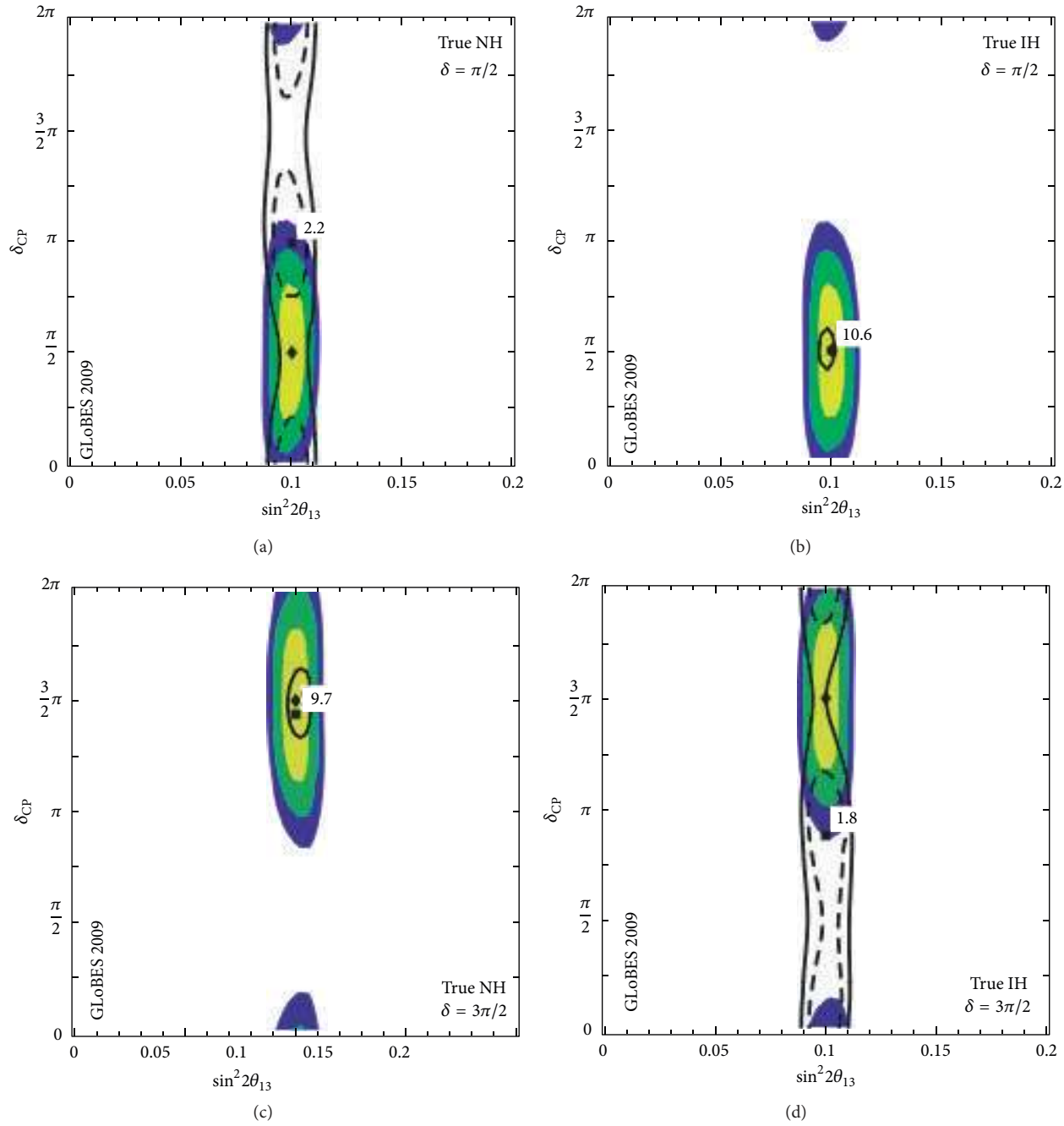

FIGURE 4: Fits in the $\theta_{13} - \delta$ plane for $\sin^2 2\theta_{13} = 0.1$, $\theta_{23} = \pi/4$, and $\delta = \pi/2$ (upper row) and $\delta = 3\pi/2$ (lower row) and a true NH (left panels) and IH (right panels), assuming the final exposure from T2K, NOvA, and DayaBay according to Table 2. The contours refer to 1σ, 2σ, and 3σ (2 dof). The fit contours for the right fit hierarchy are shaded (colored), and the ones for the wrong hierarchy fit are shown as curves. The best-fit values are marked by diamonds and boxes for the right and wrong hierarchy, respectively, where the minimum χ^2 for the wrong hierarchy is explicitly shown. Figures are based on the results of [45].

electrons is difficult and therefore one relies on signals in μ-like events, described by the expression in (10).

Early studies along these lines have been performed in [41, 59]. In Figure 5 we reproduce results obtained recently in [60, 61], where the combined sensitivity of the INO detector with data from T2K, NOvA, and DayaBay has been considered. For other recent studies see, for example, [62, 63]. It has been stressed in [42, 64] that the sensitivity to the mass hierarchy strongly depends on the ability to reconstruct the neutrino energy and direction. The second term in (10) induces characteristic features in the energy and zenith angle distribution of μ-like events. If those features can be resolved by the detector, they provide robust sensitivity to the mass hierarchy. The "low" and "high" resolution scenarios referred

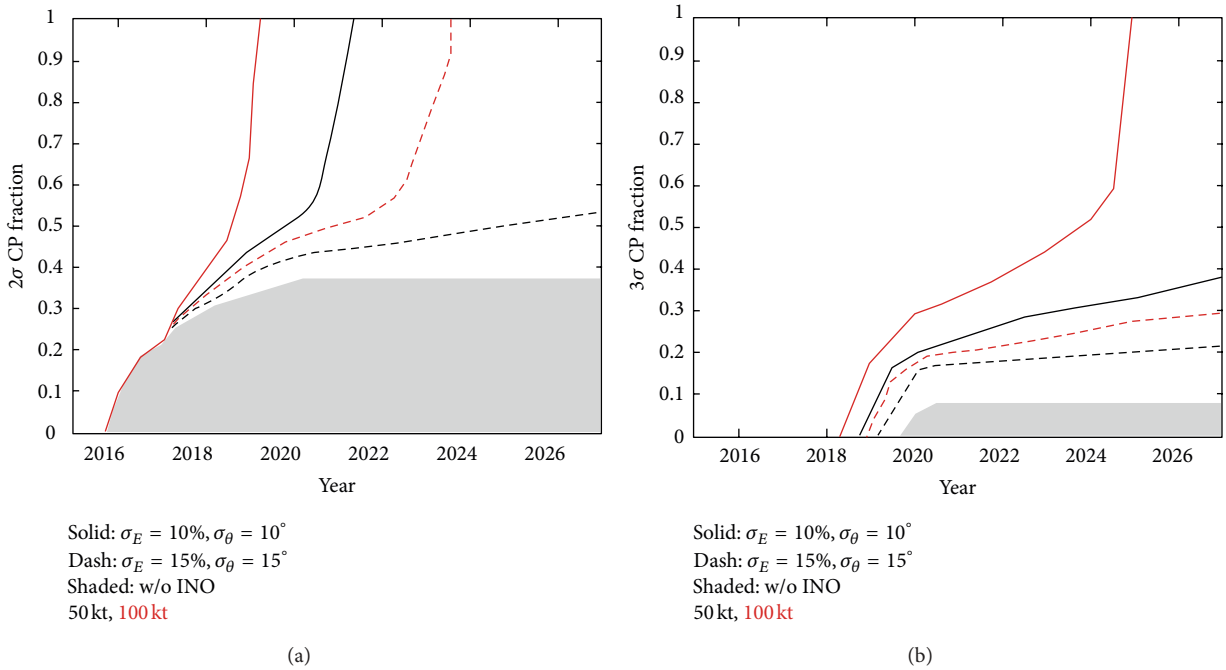

FIGURE 5: The time evolution of the fraction of values of the CP phase δ for which the combination of INO, NOvA, T2K, and DayaBay would be sensitive to the mass ordering at 2σ (a) and 3σ (b). Black (red) curves correspond to INO detector mass of 50 kt (100 kt) and dashed (solid) curves correspond to the low (high) resolution scenario; see text. The shaded area is the corresponding result without atmospheric data from INO. The true value of $\sin^2 2\theta_{13}$ has been assumed to be 0.09. Figures are based on the results of [60, 61].

to in Figure 5 assume resolutions of $\sigma_E/E_\nu = 0.15$, $\sigma_\theta = 15^\circ$ (low) and $\sigma_E/E_\nu = 0.10$, $\sigma_\theta = 10^\circ$ (high). Furthermore the sensitivity for a 50 kt or 100 kt detector is shown, which is supposed to start data taking in 2011 [55]. We observe that the sensitivity to the mass hierarchy is significantly increased compared to NOvA + T2K + DayaBay only. For all but the low resolution 50 kt detector the hierarchy can be identified for all values of δ at 2σ. However, for a 3σ determination with 100% coverage in δ the high resolution 100 kt detector seems necessary.

4.2. Atmospheric Neutrinos—Water/Argon. If charge identification is not possible (as, for instance, in water Cerenkov detectors) the effect of changing the mass hierarchy is strongly diluted by summing neutrino and antineutrino events. However, the total sample is dominated by neutrinos due to higher fluxes and detection cross-sections. Therefore the cancellation is not complete and a net effect remains between having the resonance in neutrinos or antineutrinos. Furthermore, also a statistical separation of neutrino and antineutrino events may be possible. For example, in SuperKamiokande the fraction of single and multiring events is different for neutrinos and antineutrinos, or the probability to observe a decay electron either from a muon or a pion is different [43]. On the other hand, water Cerenkov detectors can be made very big, possibly at the mega ton scale [65, 66] which may allow to explore those subtle signatures. Since for those detectors electron detection is possible, the impact of the matter effect on multi-GeV e-like events (see (9)) can be explored.

The left panel of Figure 6 shows the sensitivity to the mass hierarchy of atmospheric neutrino data in a 560 kt water Cerenkov detector, the so-called HyperKamiokande project [66]. Depending on the parameter values, a more than 3σ determination of the mass hierarchy seems possible after a few years of exposure. The figure shows that the sensitivity strongly depends on the value of θ_{23}. In general the mass hierarchy sensitivity of atmospheric neutrinos is better for larger values of $\sin^2\theta_{23}$. The same behaviour is also observed for magnetized muon detectors such as INO, see, for example, [42]. This follows from the relations given in Section 2.2, where it can be seen that effects of the oscillation probability $P_{2\nu}(\Delta m^2_{31}, \theta_{13})$—which encodes the resonant matter effects due to θ_{13} carrying the information on the hierarchy—are larger for large $\sin^2\theta_{23}$.

Many future projects for long-baseline accelerator experiments use large volume detectors which are also able to observe atmospheric neutrinos. Therefore, it is an obvious idea to explore synergies between the data from the beam and atmospheric neutrinos [67]. Figure 6 (right pannel) shows some examples, where information from beam experiments with relatively short baselines is combined with data from atmospheric neutrinos in a 440 kt water Cerenkov detector in order to resolve the mass hierarchy [68]. The beams considered there have baselines which are too short to address the mass hierarchy, and only the combination with atmospheric neutrinos allows to address this question. (Note that the combined data from the beta beam and SPL superbeam provides also some sensitivity to the hierarchy even without

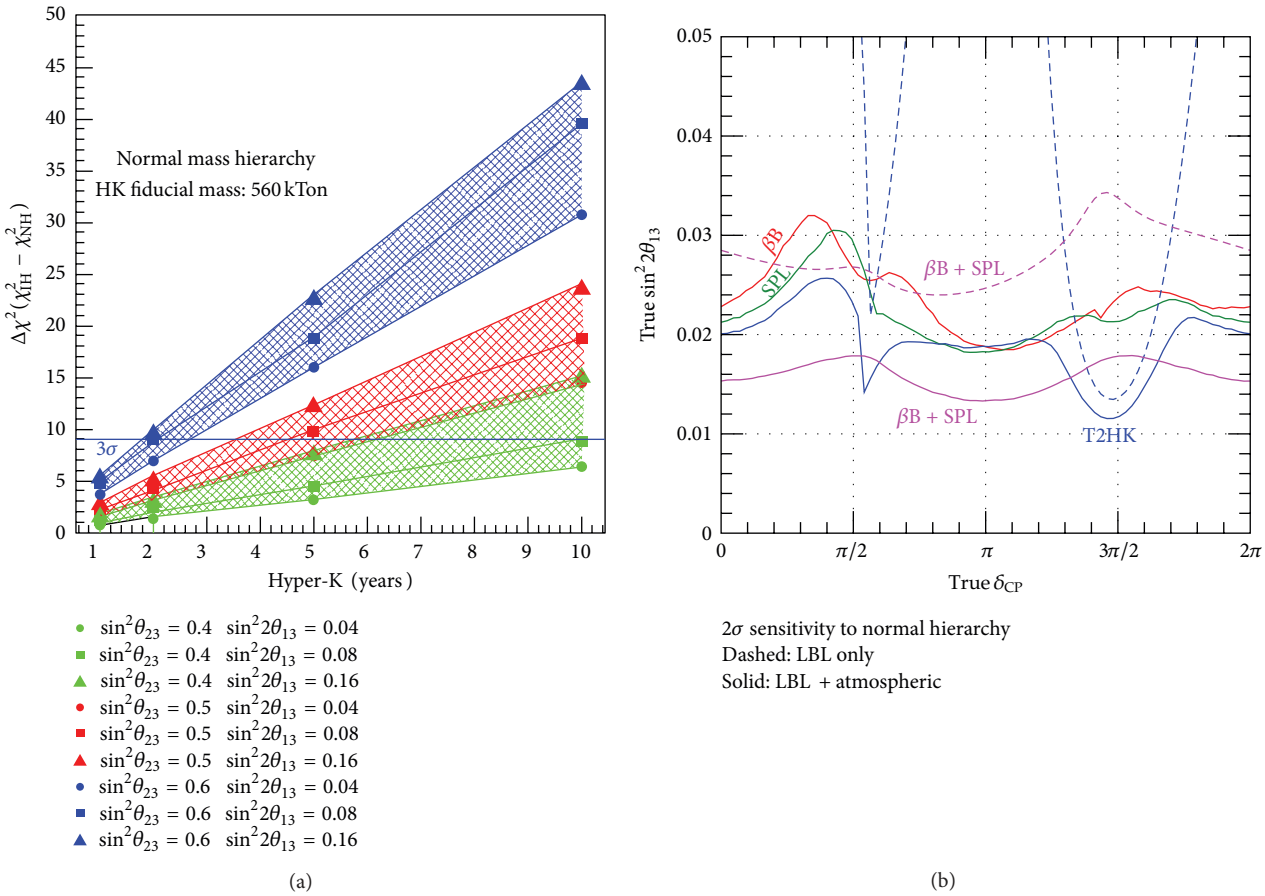

FIGURE 6: (a) Sensitivity to the neutrino mass hierarchy from Hyper Kamiokande atmospheric neutrino data. θ_{23} and θ_{13} are assumed to be known as indicated in the figure. Plot from [66]. (b) Sensitivity to the mass hierarchy at 2σ from a combination of beams at relatively short baseline with 4.4 Mt yr atmospheric neutrino data from a water Cerenkov detector. βB and SPL refer to a beta-beam and a 4 MW superbeam from CERN to Frejus (130 km), respectively, whereas T2HK corresponds to a 4 MW beam from JPARC to the HyperKamiokande detector (295 km). Dashed curves are data from beams only, and solid curves are for beams + atmospheric neutrinos. Figure is based on the results of [68].

atmospheric data (dashed magenta curve). This is based on the combination of data from $\nu_e \rightarrow \nu_\mu$ (beta beam) and $\nu_\mu \rightarrow \nu_e$ (superbeam) oscillations, which allows to break the mass hierarchy degeneracy already at first order in the parameter A (see (5)), which works already at the distance of 130 km [69]; see also [70].) Both panels in Figure 6 are based on a water Cerenkov detector, but similar results can be achieved in large (100 kt scale) liquid argon detectors [57]. We mention also that atmospheric data from such big detectors (including also the sub-GeV samples) provide excellent sensitivity to the octant of θ_{23} (see e.g., [67]) through the effects discussed already in the context of present data in Section 2.3.

4.3. Atmospheric Neutrinos—Ice. The IceCube neutrino telescope in Antarctica is able to collect a huge amount of atmospheric neutrino events. Due to the high energy threshold those data are not very sensitive to oscillations although they provide interesting constraints on nonstandard neutrino properties; see for example, [71]. With the so-called DeepCore extension [72] a threshold of around 10 GeV has been achieved, and the first results on oscillations of atmospheric neutrinos have been presented [73]; see [74] for a study on the neutrino mass hierarchy. With a further proposed extension of the IceCube detector called PINGU [75] the threshold could be even lowered to few GeV, opening the exciting possibility of a multimega ton scale detector exploring the matter resonance region. The most straight forward type of events will be muons without charge identification, and one has to rely on the huge statistic in order to identify the effect of the mass hierarchy. Below we discuss some results obtained recently in [76] focusing on the muon signal. Signatures from ν_e- and ν_τ-induced events have also been studied in [76].

In order to identify the difference between normal and inverted mass hierarchy again a crucial issue will be the ability to reconstruct the neutrino energy and direction. In Figure 7 the difference between event numbers for NH and IH (weighted by the statistical error), binned in neutrino energy E_ν and zenith angle θ_z, is shown for two assumptions on the reconstruction abilities. In the left pannel, with better resolutions, we can observe clearly the effects of the matter resonance. We note also that in different regions in the $E_\nu - \cos\theta_z$ plane the difference between NH and IH changes

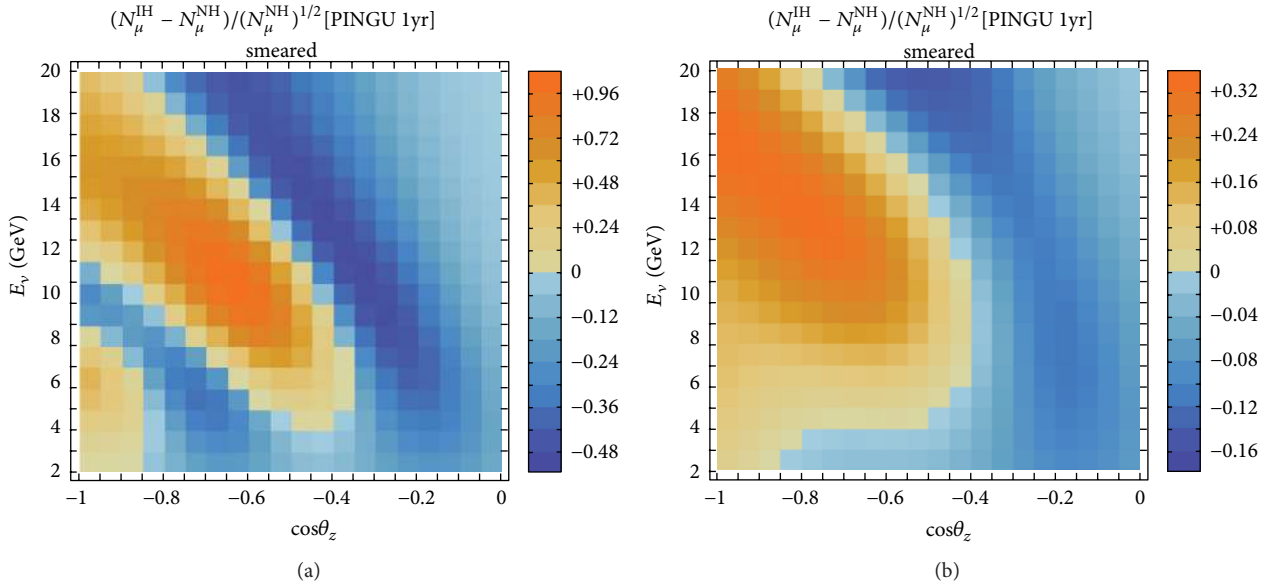

FIGURE 7: Statistical significance per bin of the difference between NH and IH for one year of PINGU data from ν_μ-induced events, binned in neutrino energy (bin width $\Delta E_\nu = 1$ GeV) and cosine of the zenith angle (bin width $\Delta \cos\theta_z = 0.05$). In the left (right) panel neutrino energy and angular reconstruction resolutions of 2 (4) GeV and 11.25° (22.5°) have been assumed. Figures from [76].

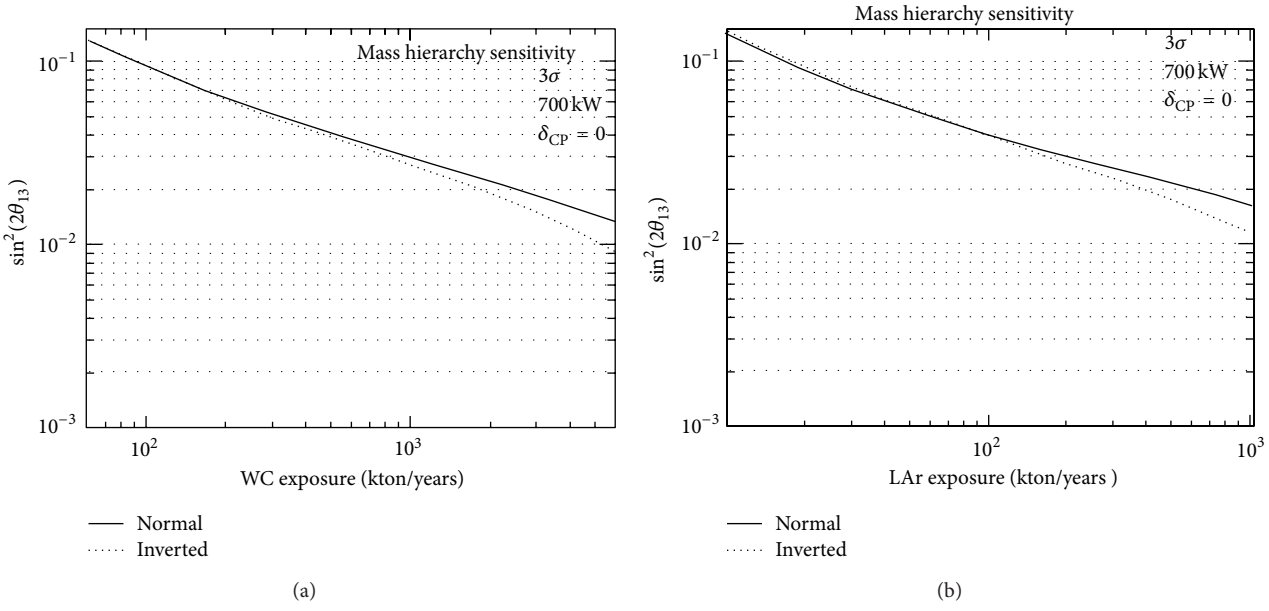

FIGURE 8: LBNE sensitivity to the mass hierarchy at 3σ as a function of the exposure for WC (a) and LAr (b) detectors. The value of δ is fixed at 0 but a similar behaviour is expected for other values of the phase. Figures taken from [103].

sign. This means that a worse resolution can easily wash out the effect. This is evident also from the right pannel, where a worse resolution has been assumed, leading to reduced significance per bin. Therefore, aiming for good energy and angular reconstruction will be an important goal in the design of the PINGU project.

Figure 7 shows the quantity $S_i \equiv (N_i^{IH} - N_i^{NH})/\sqrt{N_i^{NH}}$, where N_i^{NH} (N_i^{IH}) is the number of μ-like events in the case of NH (IH) in a given bin i. Hence, S_i corresponds to the statistical significance (in number of standard deviations) per bin. In the absence of systematical errors the total significance is given by $\sqrt{\sum_i S_i^2}$, and the configurations considered in Figure 7 would lead to sensitivities at the level of 16σ (left pannel) or 7σ (right pannel) [76]. Hence, considering only statistical errors, excellent sensitivity to the mass hierarchy is obtained already after one year of PINGU data. Those very

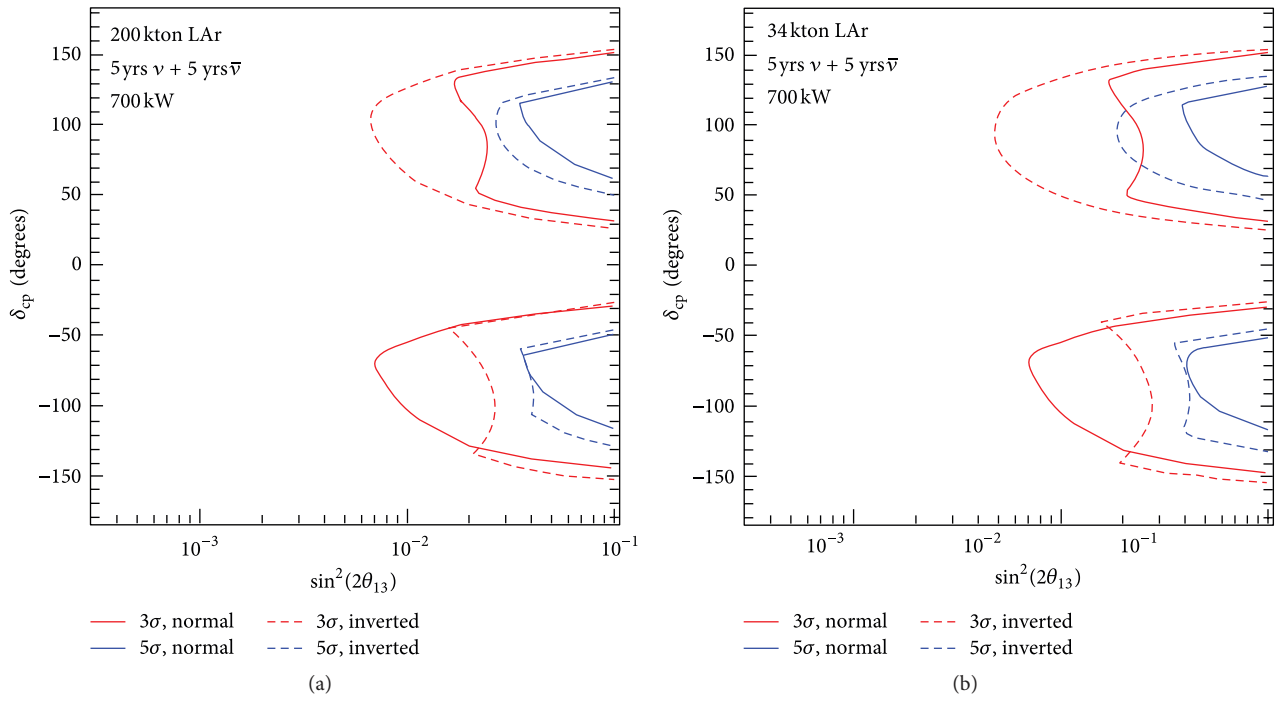

FIGURE 9: LBNE sensitivity to CPV at 3σ (red curves) and 5σ (blue curves) for 5 years of running in the neutrino channel plus 5 in the antineutrino one. A 200 kton WC (a) or a 34 kton LAr (b) are used in a 700 kW beam. Figure is taken from [103].

promising results are yet to be supported by detailed studies on the achievable energy and angular reconstruction as well as realistic investigations of systematical uncertainties.

4.4. Mass Hierarchy from Reactors. All the possibilities to identify the neutrino mass hierarchy discussed above are based on the matter effect in oscillations due to θ_{13}. In [77] an alternative has been pointed out, based on oscillations of reactor neutrinos, where matter effects are negligible. The three-flavour survival probability of $\overline{\nu}_e$ in vacuum is easily obtained as

$$\begin{aligned} P_{\nu_e \to \nu_e} &= 1 - \cos^4\theta_{13}\sin^2 2\theta_{12}\sin^2\left(\frac{\Delta m^2_{21}L}{4E}\right) \\ &\quad - \sin^2 2\theta_{13} \\ &\quad \times \left[\cos^2\theta_{12}\sin^2\left(\frac{\Delta m^2_{31}L}{4E}\right) + \sin^2\theta_{12}\sin^2\left(\frac{\Delta m^2_{32}L}{4E}\right)\right]. \end{aligned} \tag{11}$$

The spectrum of reactor experiments ranges from neutrino energies of about 1.3 MeV to 12 MeV with a peak around 4 MeV. Consider now a baseline $L \simeq 60$ km. Then we obtain for the arguments of the oscillating terms:

$$\begin{aligned} \frac{\Delta m^2_{21}L}{4E} &\approx \frac{\pi}{2}\left(\frac{E}{4\,\text{MeV}}\right)^{-1}, \\ \frac{|\Delta m^2_{31}|L}{4E} &\approx \frac{|\Delta m^2_{32}|L}{4E} \approx 50\left(\frac{E}{4\,\text{MeV}}\right)^{-1}. \end{aligned} \tag{12}$$

Hence, considering the spectrum obtained in a reactor experiment at about 60 km, the first term in (11) gives a "slow" oscillation in $1/E$, with a large amplitude of $\cos^4\theta_{13}\sin^2 2\theta_{12} \approx 0.8$. These are the oscillations due to the "solar" frequency as observed by the KamLAND experiment. For an experiment at 60 km the first minimum of the survival probability occurs close to $E \sim 4$ MeV, at the peak of the expected number of events.

The terms in the second line of (11) lead to fast oscillations in $1/E$ (see (12)) on top of the slow "solar" oscillation, with a small amplitude proportional to $\sin^2 2\theta_{13} \approx 0.1$. As evident from (11) there are actually two fast frequencies, one due to Δm^2_{31} and one due to Δm^2_{32}, which differ by Δm^2_{21} (about 3%). The sensitivity to the mass hierarchy appears as follows. First, note that depending on the hierarchy we have $|\Delta m^2_{31}| > |\Delta m^2_{32}|$ for NH or $|\Delta m^2_{31}| < |\Delta m^2_{32}|$ for IH. Second, the amplitudes of the two fast frequencies are different because of the nonmaximal value of θ_{12}: the amplitude of the Δm^2_{31} frequency is $\sin^2 2\theta_{13}\cos^2\theta_{12} \approx 0.07$ while the one of the Δm^2_{32} frequency is $\sin^2 2\theta_{13}\sin^2\theta_{12} \approx 0.03$. Hence, if an experiment can measure the fast frequencies and find out which one of

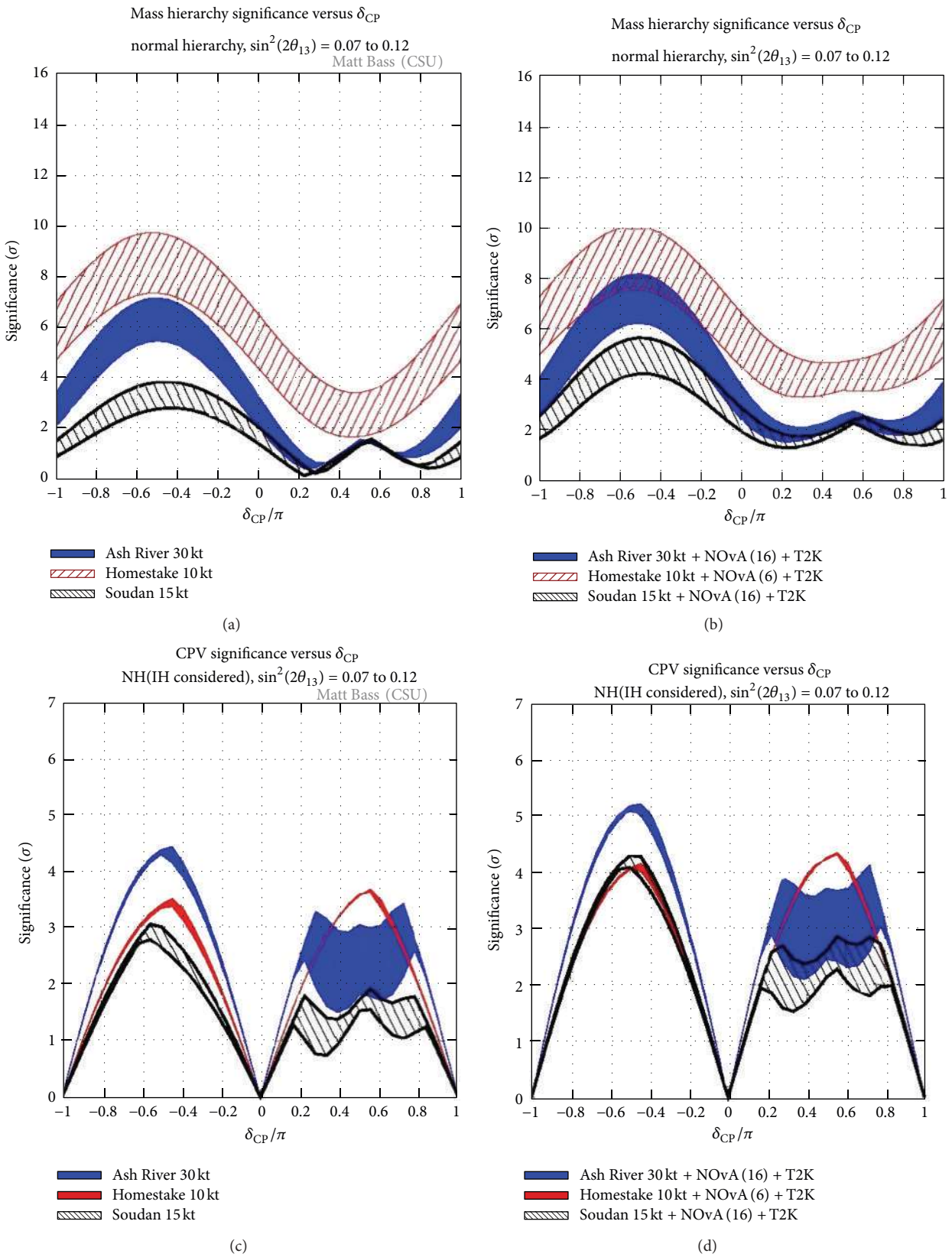

FIGURE 10: LBNE sensitivity to the mass hierarchy (upper plots) and CPV (lower plots) at 3σ as a function of δ for the three reconfiguration options, as described in the text. The sensitivities are reported for the experiment alone (left) and when combined with NOvA for $3\nu + 3\overline{\nu}$ years and T2K. The Ash River and Soudan options use the NuMI beam line, and therefore additional $5\nu + 5\overline{\nu}$ years for NOvA are included, assuming that this detector will be kept in operation in parallel to the LAr detector. Figure taken from [104].

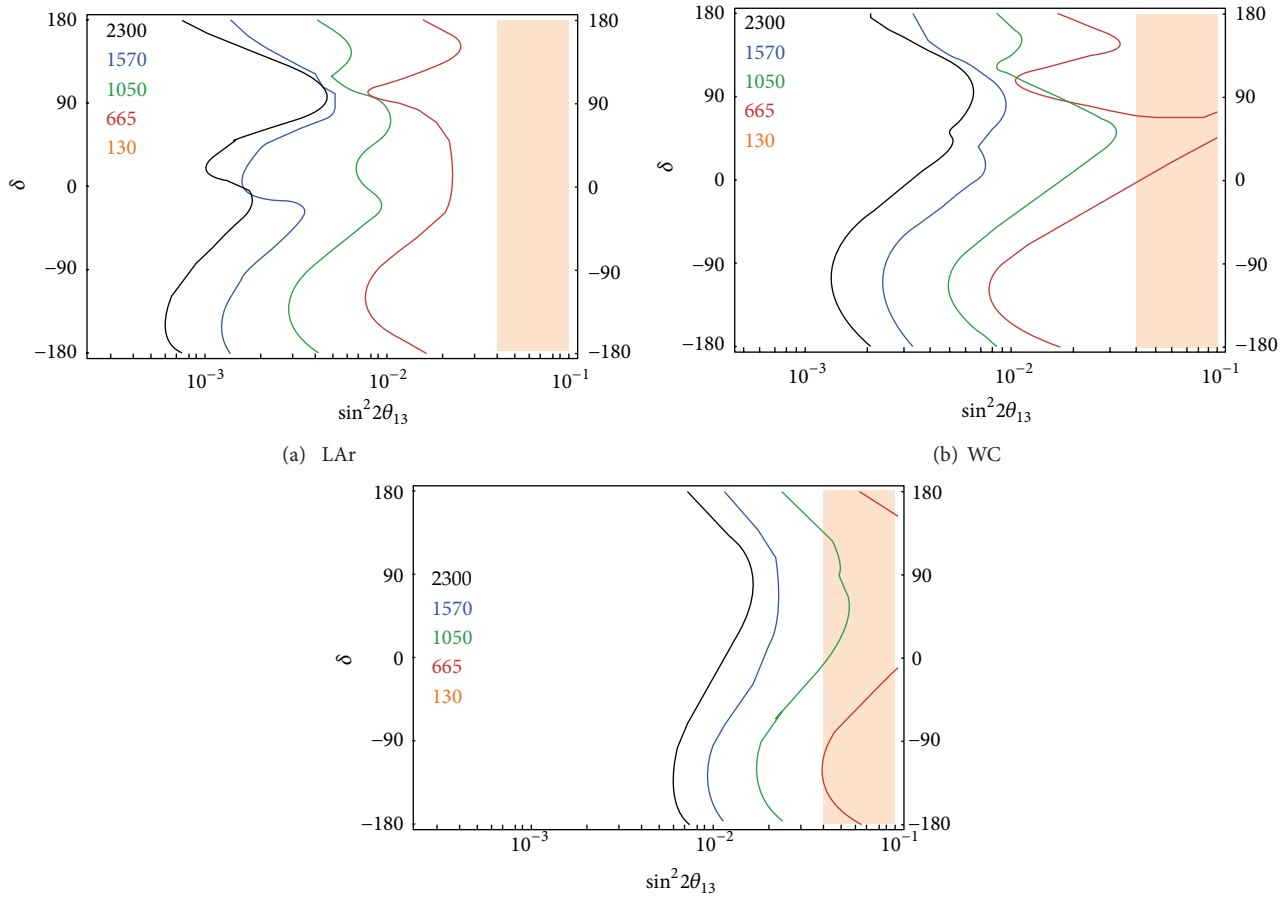

(a) LAr (b) WC

(c) LSc

Figure 11: LAGUNA hierarchy discovery at 3σ as a function of $\sin^2 2\theta_{13}$ and δ. The different lines correspond to different baselines, as indicated in the legend in km. The details of the beams used are reported in the text. The detectors are 100 kton LAr TPC, 50 kton LSc, and 440 WC detector. The shaded region reports the 3σ allowed values from Daya Bay. Figure is taken from [107].

the two fast frequencies has the larger amplitude (the larger or the smaller frequency), the mass hierarchy is determined. The effect can be illustrated by performing a Fourier transform of the event spectrum, where the two frequencies appear as a high and low peaks in the transformed spectrum [78].

The experimental requirements are obvious from the above discussion: (i) a good energy resolution is required in order not to wash out the fast oscillations and (ii) because of the small amplitude of the fast oscillations one needs enough statistics to be able to establish their presence. Numerical studies have been performed in [78–80]. The results of [80] indicate that exposures of order few 100 kt GW yr and energy resolutions of order 3% are required, which makes this measurement challenging. (We recall that the KamLAND experiment has about 1 kt, the LENA proposal [65] is for 50 kt, and typical modern reactor neutrino experiments have an energy resolution of 5-6%.) The DayaBay collaboration has identified a suitable detector location at a distance of 60 km to several reactor cores with a total of 17.4 GW power (and another 17.4 GW in the planning stage) and is pursuing the possibility of a mass hierarchy measurment as the DayaBay-II project [81]. Let us also mention that such a big reactor experiment at 60 km would provide ultimate precision on the determination of θ_{12} and Δm^2_{21}; see, for example, [82].

5. High-Precision Long-Baseline Facilities

As discussed above, the next generation of neutrino experiments will have some sensitivity to matter effects, and it may be possible to have the mass hierarchy determined by 2025. The search for CP violation is more challenging, and it is unlikely that its discovery can be achieved in the same time frame. Upgraded long baseline experiments with larger statistics and better control of systematics will be needed.

In order to understand how these experiments will be sensitive to CP violation and will achieve precise measurements of the oscillation parameters, let us consider the approximate formula for the oscillation probability $P_{\nu_\mu \to \nu_e}$ given in (3). The first term in the probability is the "atmospheric term" which is dominant as θ_{13} is large, $\sin^2 2\theta_{13} \approx 0.09$. This is the term which is most sensitive to matter effects and drives the ability of coming and next-generation experiments to establish the mass hierarchy. The second line is the "CP term" which contains the dependence on the

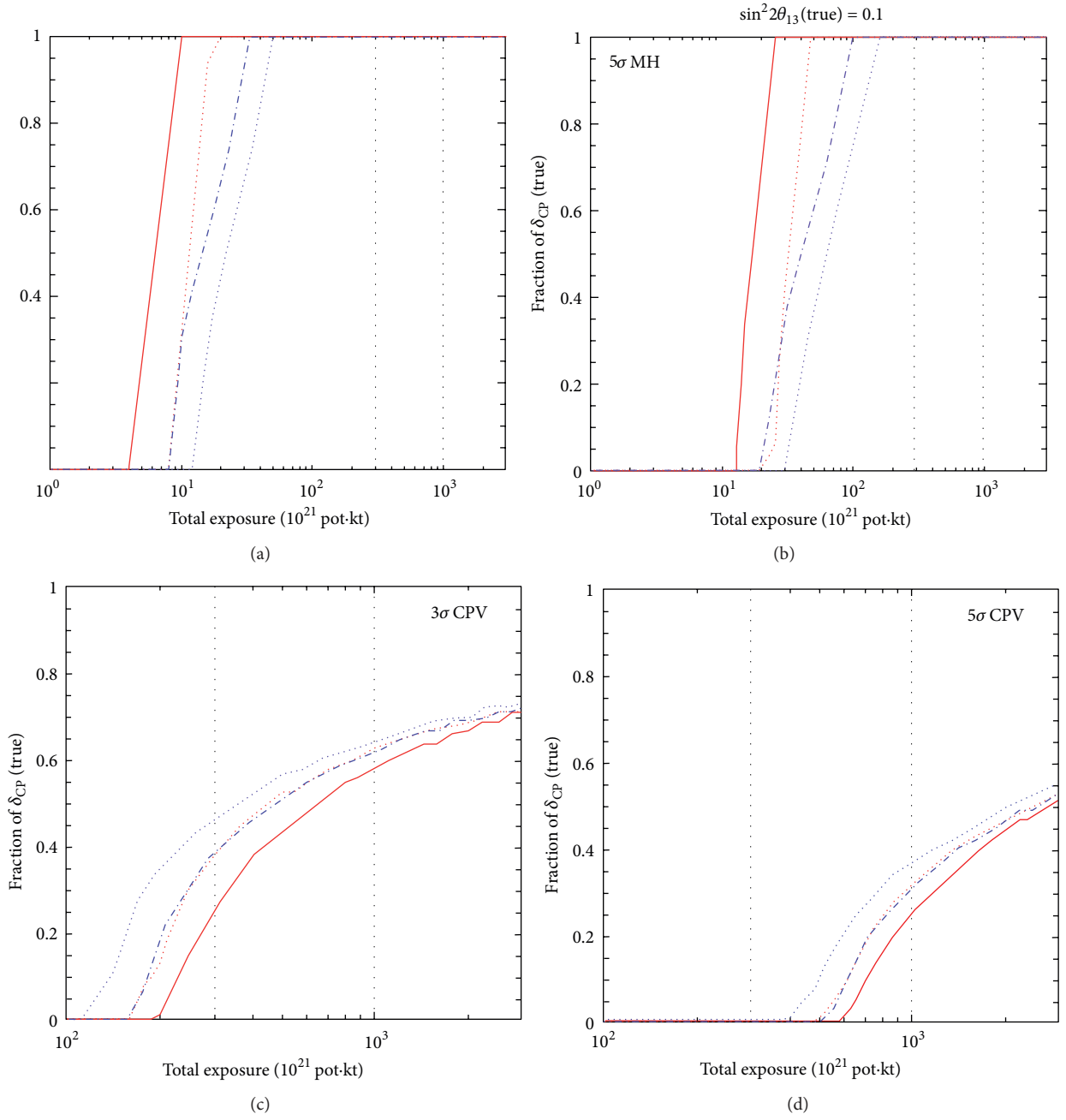

FIGURE 12: CP fraction for which a mass hierarchy (upper plots) and CP violation (lower plots) discovery at 3σ (left) and 5σ (right) is possible as a function of exposure for a staged LAGUNA setup. The different lines correspond to true normal (inverted) hierarchy for solid (dashed) lines and for a baseline of 2290 km (1540 km) for red (blue) lines. Figure is taken from [112] where more details about the simulations can be found.

CP violating phase δ. As we see, this term becomes more important at lower energies, and for this reason access to the low energy part of the spectrum is critical to achieve good sensitivity to CP violation. It should also be noted that for large θ_{13} the "CP term" is a small correction with respect to the dominant "atmospheric term," and in fact the CP asymmetry, defined as $(P_{\nu_\mu \to \nu_e} - P_{\overline{\nu}_\mu \to \overline{\nu}_e})/(P_{\nu_\mu \to \nu_e} + P_{\overline{\nu}_\mu \to \overline{\nu}_e})$, scales as $\sin^{-1}\theta_{13}$ and is suppressed for large θ_{13}. Therefore, despite the fact that large θ_{13} implies large number of events at future LBL facilities, the discovery of CP violation remains very challenging and requires precise measurements of the probabilities, with small statistical and systematic errors, (It has been shown that CP violation can also be searched for in short baseline experiments, such as (a Decay-At-rest Experiment for CP studies At the Laboratory for Underground Science) [83] DAEδALUS. This uses high-power proton accelerators to produce a $\overline{\nu}_\mu$ beam with energies in the few tens of MeVs. The appearance oscillation $P_{\overline{\nu}_\mu \to \overline{\nu}_e}$ will be detected via inverse beta decay by a large WC detector doped with gadolinium, to reduce the backgrounds, or scintillator

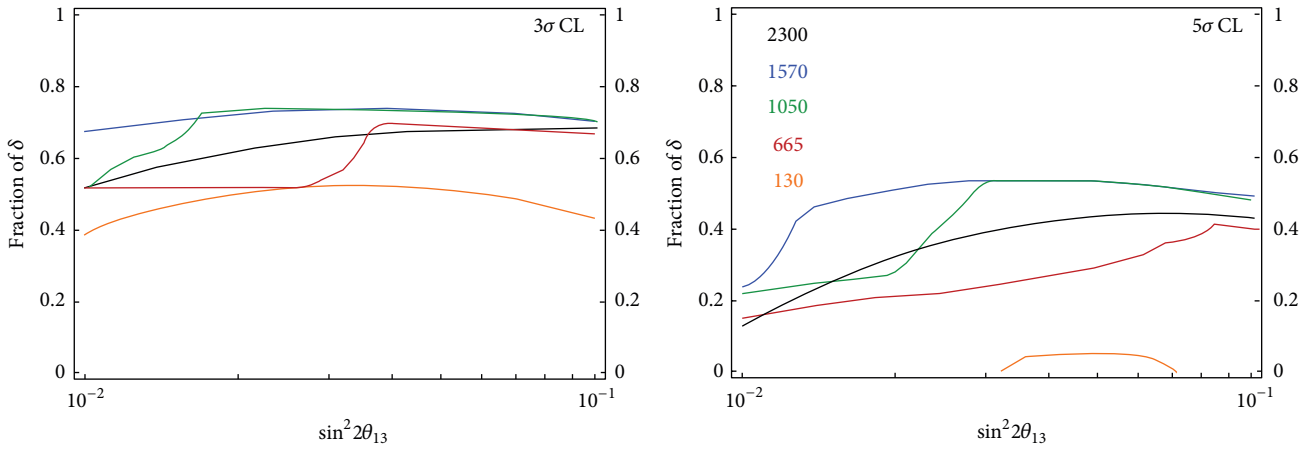

FIGURE 13: LAGUNA CP fraction for which a CP violation discovery at 3σ (left) and 5σ (right) is possible as a function of $\sin^2 2\theta_{13}$ for the LAr (upper plots) and WC (lower plots) detector. Figure is taken from [107].

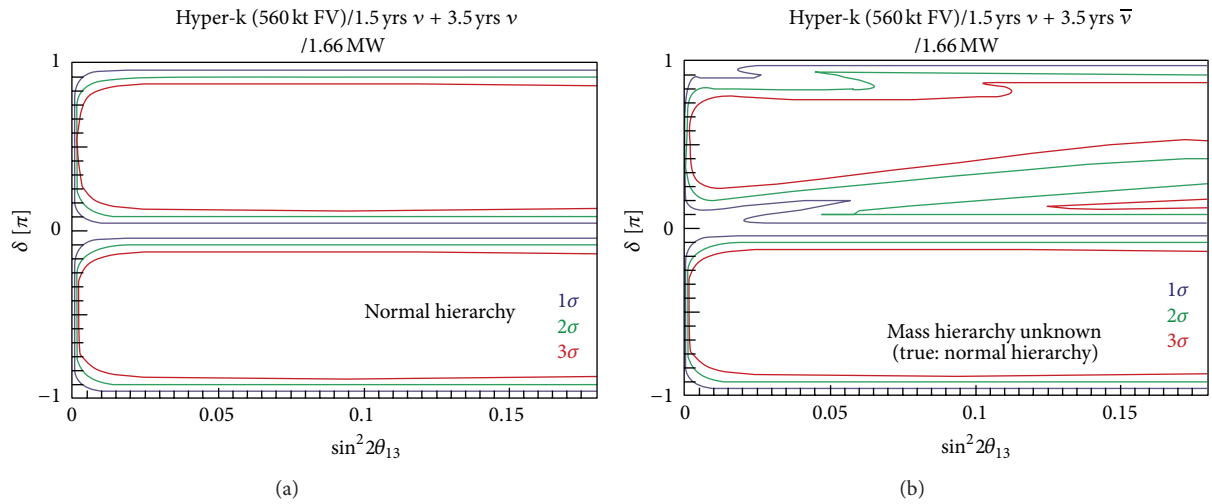

FIGURE 14: T2HK sensitivity to CP violation at 1, 2, and 3σ as a function of $\sin^2 2\theta_{13}$. The mass hierarchy is assumed known (a) or not (b). Figure is taken from [66].

detectors. Further details are provided elsewhere in this volume).

Moreover, as it can be seen from the probability equation, CP-violating and matter effects are entangled, and the extraction of the parameters of interest, namely, the $\mathrm{sgn}(\Delta m^2_{31})$, the phase δ, and θ_{23}, is affected by the widely studied problem of degeneracies: different sets of parameters give the same probabilities in the neutrino and in the antineutrino channels at fixed L/E [20, 29, 47, 84, 85]. Therefore, even a very precise reconstruction of the probabilities does not allow to determine the true parameters, and the physics reach is severely affected. In vacuum three degeneracies can be identified. (i) The intrinsic degeneracy: θ_{13}, δ have fake solutions which strongly depend on energy. For large θ_{13} and in vacuum, the "fake" solutions are given by [84]

$$\theta'_{13} \simeq \theta_{13} + \cos\delta \sin 2\theta_{12} \frac{\Delta m^2_{21} L}{4E} \cot\theta_{23} \cot\left(\frac{\Delta m^2_{21} L}{4E}\right). \quad (13)$$

(ii) The sign degeneracy: in absence of matter effects, it is possible to change the sign of Δm^2_{31} and δ to $\pi - \delta$ without affecting the probabilities. In matter this degeneracy is broken. (iii) The octant of θ_{23}: if the angle is not maximal as currently suggested by the data, see Section 1.

The problem of degeneracies has significant impact on the precision of the oscillation parameter measurements, and in particular on the ability to establish CP violation. A lot of effort has gone into devising strategies to weaken the impact of the degeneracies; see, for example, [47, 70, 86–102]. Long enough baselines (>800–1000 km) have strong matter effects and can be used to solve the sign degeneracy; information at several energies, for example, by using wideband beams, is important, with the one coming from the low-energy part of spectrum being critical for CP violation and the octant degeneracy. Other techniques have also been explored, for example, combining different channels which have different

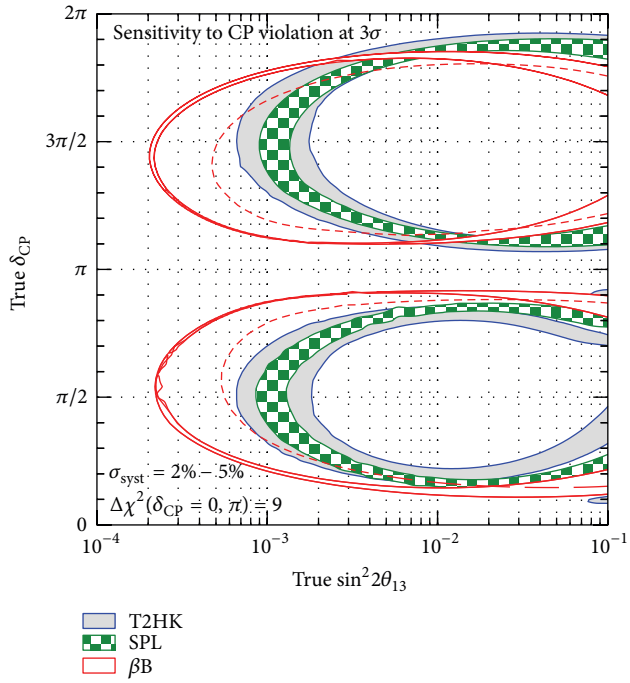

FIGURE 15: CP violation discovery at 3σ as a function of δ for a betabeam, SPL, and T2HK. The combination of SPL and a betabeam is also shown. The betabeam lines correspond to $5.8(2.2) \times 10^{18}$ decays per year of ^{6}He (^{18}Ne). Details of the simulations can be found in [68]. The width of the bands reflects the change of the systematic errors from 2% to 5%. The dashed curves are obtained for a betabeam flux reduced by a factor of two.

dependence on the parameters, or different baselines and/or typical energies. Several of these studies have been performed focusing on small values of θ_{13}. Thanks to the large value of θ_{13}, some of the degeneracies become less important or more easily solved. For instance, determining the mass hierarchy will be easier than previously expected, and it is even possible that it will be achieved prior to the start of the next generation of long baseline experiments, as discussed in Section 4.

In this section we briefly review future LBL experiments which will provide improved sensitivity to the mass hierarchy and CP violation and the possibility to measure with various degree of precision the oscillation parameters. Several type of setup are under consideration, some of them being at the design study or proposal level and others more advanced: superbeams (LBNE, T2HK, LAGUNA-LBNO), betabeams, and neutrino factory (NF). In the following, we briefly review these three different types of facilities. We focus on their physics reach and we defer the readers to the relevant chapters in this volume for a detailed description of the experimental facilities.

5.1. Future Superbeams. Superbeams are based on currently used technology and require an upgrade in neutrino flux and detector size. The beam is constituted mainly by muon neutrinos which are produced by pion and kaon decays. The experiments search for the $\nu_\mu \rightarrow \nu_\mu$ probability, sensitive to Δm^2_{31} and θ_{23}, and, importantly, for the subdominant oscillation $\nu_\mu \rightarrow \nu_e$. Detectors with excellent ν_e reconstruction are needed, the technologies of choice being Water-Cherenkov, Liquid Argon (LAr), or scintillator (LSc) ones. A wide range of energies is currently under consideration, going from 200 MeV of SPL to several GeVs for CN2PY (CERN to Pyhäsalmi), with corresponding distances from 100 km to 2300 km. The detector can be located on-axis or off-axis: in the first case it sees a wide spectrum, while in the latter the beam is peaked at low energies and its high energy tail is suppressed. They typically have an excellent reach for the mass hierarchy, if $L > 1000$ km or so, and very good sensitivity to CP violation. The main limiting factor is the intrinsic ν_e contamination of the beam, at a level of 0.5%–1%. Another very important experimental issue is the background due to the misidentified π^0 produced in neutral current (NC) interactions, as one of the γs from the pion decay $\pi^0 \rightarrow \gamma\gamma$ is missed. This background is particularly important at low energies for CP violation searches and impacts differently beams at different energies and with different detectors; for instance, LAr ones have an excellent NC rejection. For the antineutrino channel, a significant contribution to the signal and background can also come from the ν_μ and ν_e components of the beam, in absence of detector magnetisation. Systematic errors are an important factor: for large θ_{13}, as the "atmospheric term" dominates the appearance oscillation probability, those on the signal are more relevant than those on the backgrounds and need to be controlled at the few % level. Various superbeam options are under study or being proposed for the future.

LBNE [103]*:* in the US the Long-Baseline Neutrino Experiment (LBNE) is the most advanced proposal for a next generation long baseline option. According to the 2010 LBNE Interim Report [103], the beam is sourced at the Main Injector at Fermilab using a new neutrino beamline with 700 kW of power. Its main requirements include a broad beam which covers both first and second oscillation maxima located at 2.4 and 0.8 GeV, respectively, an increased flux at low energy in order to compensate for the lower detection cross the sections, a suppression at energies above 5 GeV in order to reduce the NC backgrounds which pile up at low energy, and the lowest level of ν_e contamination possible. The detector is located at the DUSEL site, at a distance of 1300 km from Fermilab. Various options were contemplated in the 2010 LBNE Interim Report: two or three 100-kton fiducial mass Water Cherenkov detectors with 15% or 30% PMT coverage and with or without gadolinium loading, or multiple 17-kton fiducial mass LAr detectors or a combination of them. The location could be at 4850, 800, or 300 feet depth, depending on the emphasis put on nonaccelerator physics, such as proton decay, supernova, and other astrophysical neutrinos. The experiment was assumed to run for 5 years in neutrinos and 5 in antineutrinos. In this configuration, it could achieve the determination of the mass hierarchy in less then a year at 3σ as shown in Figure 8. LBNE could also have very good sensitivity to CP violation with a 60% coverage at 3σ in the allowed range of values of $\sin^2 2\theta_{13}$, for a 200 kton Water Cherenkov or 34 kton LAr detectors, see Figure 9.

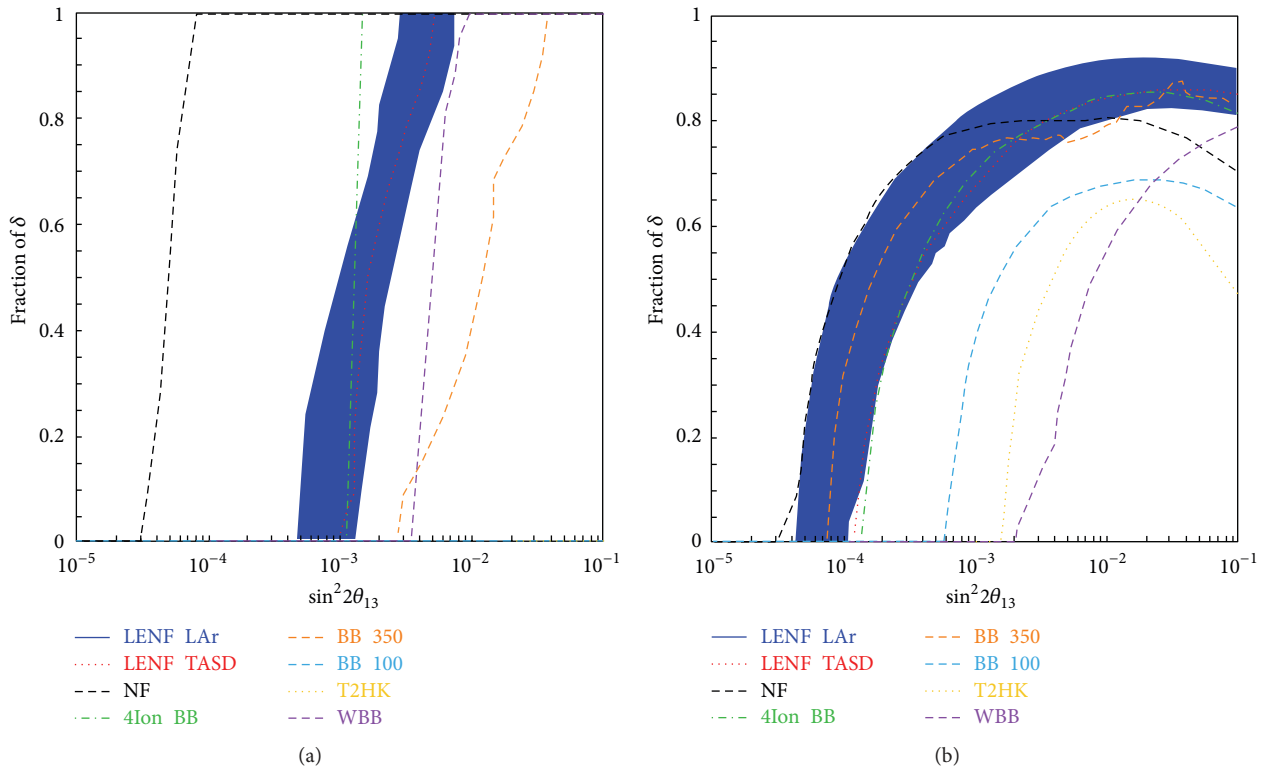

FIGURE 16: (a) 3σ sensitivity to the mass hierarchy, in terms of the fraction of δ values for which $\delta = 0, \pi$ can be excluded, as a function of $\sin^2 2\theta_{13}$ with a LENF with 20 kton TASD, LENF with 100 kton LAr detector (the band corresponds to the varying detector performance), high energy neutrino factory, a wide band beam, 3 betabeam configurations and for T2HK. Figure is taken from [144] where further details of the simulations are reported. (b) Same as the left but for CP violation.

In 2011, the technology choice was made, favouring a LAr detector thanks to its excellent performance in energy resolution, efficiency, and background reduction for the range of energies of interest. In 2012, due to funding restrictions, the LBNE configuration was reconsidered, and a severe reduction of the detector size was necessary at a first stage, keeping open the possibility of an upgrade to a large/multiple detector at a later time. Three options were considered for the first step: (i) a beam from the the existing NuMI beamline in the low-energy configuration with a 30-kton LAr detector located at the surface 14 mrad off-axis at Ash River in Minnesota, $L = 810$ km, (ii) using the beam above but with a 15-kton detector at the Soudan mine in Minnesota, $L = 735$ km as MINOS, (iii) a new low-energy LBNE beamline aimed at a 10-kton LAr detector at Homestake (on-axis) in South Dakota, $L = 1300$ km. A report by the Steering Committee [104] was prepared and the reach of each option is analysed in detail, see Figure 10. The report favoured option (iii). This configuration offers the best opportunities for a long-term programme with a 20–25 kton underground detector at Homestake and a Project X sourced beam. The recommendation was very well received and on 29 June 2012 DOE confirmed that CD1 will be reviewed towards the end of October 2012.

LAGUNA-LBNO (CN2PY) [105–107]: in Europe a next-generation superbeam experiment with a beam sourced at CERN is being considered in the LAGUNA and LAGUNA-LBNO FP7 Design Studies, funded by the European Commission. The LAGUNA project, which is finished in 2011, considered seven possible locations for a European large underground laboratory which could host a megaton-scale detector for neutrino, astroparticle physics, and proton decay searches. The Design Study focussed on site investigations and on the development of the design of a facility for the neutrino underground observatory. Three detector technologies were considered: 100 kton liquid argon [108], 50 kton liquid scintillator [109, 110], and 440 kton Water Čerenkov [111] detectors. The study concluded that all locations would in principle allow to host the facility. Importantly, the chosen detector could also be the target for a superbeam from CERN. Depending on the site, the available distances, see Table 3, range from 130 km for Fréjus to 2300 km for Pyhäsalmi, the longest baseline considered at present for superbeams. The Design Study LAGUNA-LBNO, which started in October 2011, is further developing the study of the beam and the physics reach of the long baseline setup, with focus on the CERN to Pyhäsalmi option for the first phase and various options for a second stage.

A detailed study of the sensitivity to the mass hierarchy and CP violation has been performed in [107]. In the lowest energy configuration of the beam (the $L = 130$ km baseline), the simulation assumed 5.6×10^{22} protons on target (PoT) per year, with an energy of 4.5 GeV, for 2 (8) years of running for neutrino (antineutrinos). In the multi-GeV regime, used for baselines with $L > 130$ km, the CERN high-power PS2

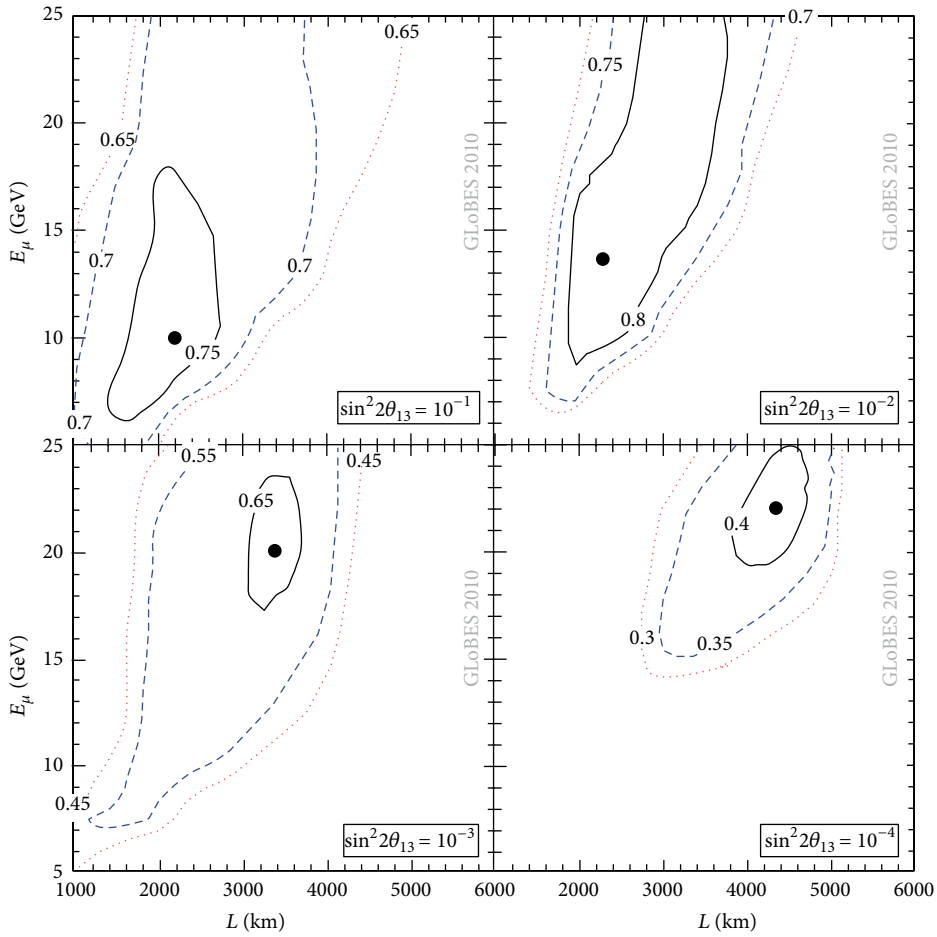

FIGURE 17: Fraction of the values of δ for which there is sensitivity to CP violation at 3σ as a function of L and muon energy. A single baseline Neutrino Factory is used with a 50 kton MIND detector. The optimal performance is marked by a dot. Figure is taken from [147].

TABLE 2: Summary of the "nominal" luminosities for the current generation of reactor and beam experiments. See [45] for details.

Setup	t_ν [yr]	$t_{\bar{\nu}}$ [yr]	P_{Th} or P_{Target}	L [km]	Detector technology	m_{Det}
Double Chooz	—	3	8.6 GW	1.05	Liquid scintillator	8.3 t
Daya Bay	—	3	17.4 GW	1.7	Liquid scintillator	80 t
RENO	—	3	16.4 GW	1.4	Liquid scintillator	15.4 t
T2K	5	—	0.75 MW	295	Water Cerenkov	22.5 kt
NOvA	3	3	0.7 MW	810	TASD	15 kt

configuration was considered with 3×10^{21} PoT per year with 50 GeV, corresponding to 2.4 MW with 10^7 useful second per year (or 1.6 MW assuming 1.5×10^7 seconds per year). Given the large value of θ_{13}, most of the configurations can determine the ordering of neutrino masses at high confidence level, as shown in Figure 11, with increased sensitivity for longer baselines. In view of this, the possibility of staging the detector, starting from a "pilot" detector of 10 to 20 kton mass, to be later upgraded to reach the baseline configuration of 100 kton, has been considered [112]. The study shows that the mass hierarchy can be reached in few years of data taking; see Figure 12.

These setups can also provide excellent sensitivity to CP violation both for the short baselines with a Water Cherenkov detector and the longer ones with a LAr detector. The LSc option could provide similar reach but only if the NC background could be controlled at a similar level. Current studies seem to indicate that NC could not be rejected at more than the 10%–20% level, severely affecting the sensitivity to CP violation for this type of detector. Typically, for the relevant range of values of θ_{13}, CP violation can be established at 3σ for ~70% of the values of δ phase and good reach is obtained even at the 5σ level; see Figures 12 and 13. It should be noted that sufficiently long baselines, such as the 2300 km

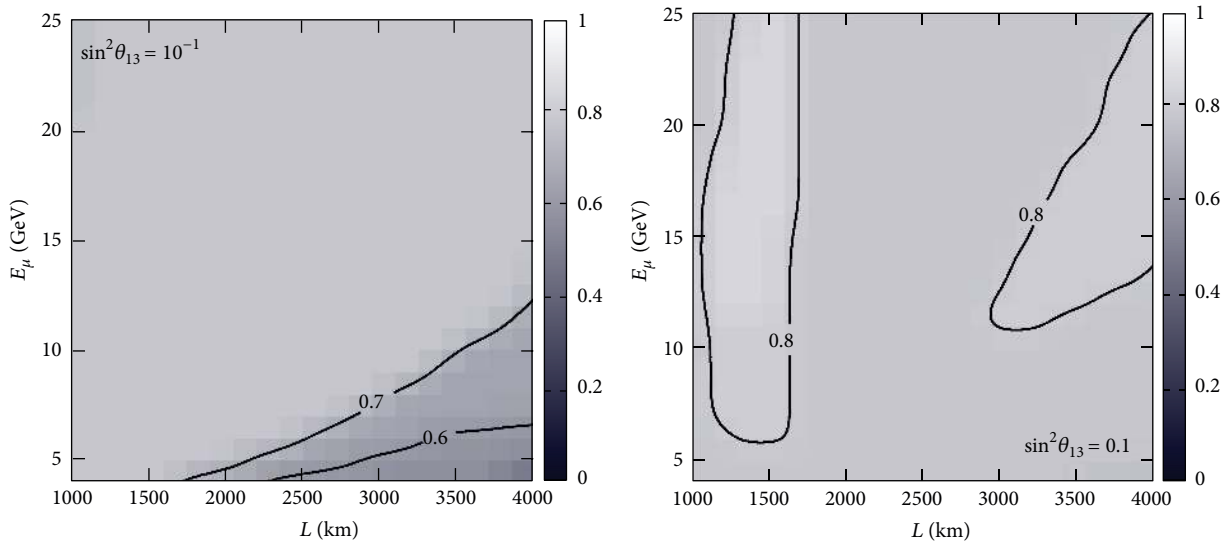

Figure 18: CP violation discovery at 3σ fraction as a function of baseline, L, and stored-muon energy using the TASD detector (a) and LAr one with optimistic performance (b). The lines indicate the fraction of values of δ for which sensitivity can be achieved. Further details can be found in [148] from which the figures have been taken.

Table 3: The seven potential locations for an underground neutrino observatory under consideration in the LAGUNA Design Study: the distance from CERN and the energy of the first oscillation maximum, in the absence of matter effects, are given. From [106].

Location	Distance from CERN [km]	1st osc max [GeV]
Fréjus (France)	130	0.26
Canfranc (Spain)	630	1.27
Umbria (Italy)	665	1.34
Sierozsowice (Poland)	950	1.92
Boulby (UK)	1050	2.12
Slanic (Romania)	1570	3.18
Pyhäsalmi (Finland)	2300	4.65

one, and a broad spectrum with good energy resolution allow to have an excellent separation of the asymmetry due to matter effects (i.e., the mass hierarchy measurement) and the CP asymmetry and thus to break the parameter degeneracies discussed above. Therefore, the existence of matter and CP violation-induced effects will be tested explicitly, without overrelying on theoretical modelling and assumptions.

J-PARC to Hyper-Kamiokande long baseline experiment (T2HK) [66]*:* recently a letter of intent (LoI) has been published for a long baseline experiment which uses a 1.66 MW beam from the J-PARC accelerator to a 1 Mton Water Cherenkov detector located 2.5° off-axis at 295 km distance in the Kamiokande site. Its main goal is the discovery and/or measurement of CP violation in the leptonic sector. One of the advantages of this configuration is the excellent energy resolution provided by the WC detector at these energies, the large number of events, and, thanks to the off-axis location and the beam configuration, the low level of intrinsic background, <1%. A running of 1.5 (3.5) years for neutrinos (antineutrinos) is assumed, with one year given by 10^7 seconds. Systematic errors play an important role and, based on foreseen improvements with respect to T2K, a level of 5% is assumed for the neutrino flux uncertainty, the neutrino interaction cross-section, the near detector efficiency, and the far detector systematics. The baseline is too short to provide a good reach for the mass hierarchy, with some sensitivity only for favourable values of δ. Additional information can be obtained from atmospheric neutrino events [67], as discussed in Section 4. The knowledge of the mass hierarchy plays an important role as it cannot be determined by the experiment itself but can induce significant degeneracies for large θ_{13}. If the mass hierarchy is known, CP violation can be established at 3σ for ~70% of the values of δ for $\sin^2 2\theta_{13} > 0.03$. In the opposite case, there is a loss of ~20% of the coverage in δ for $\sin^2 2\theta_{13} = 0.1$. A summary of the reach is reported in Figure 14.

SPL [68, 113]*:* another superbeam configuration is under consideration in Europe within the EUROnu Design study. This setup exploits a 4 MW beam to produce a very low energy superbeam aimed at a 440 kton MEMPHYS Water Cherenkov detector located 130 km away at Fréjus. The very high intensity of the beam and very large detector compensate

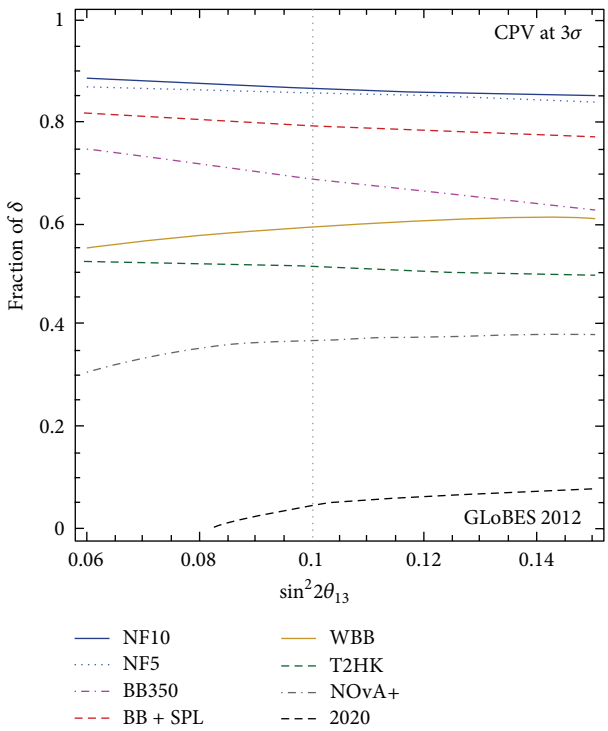

FIGURE 19: δ-fraction for 3σ CP violation sensitivity for an upgrade of NOvA with a 30 kton LAr detector (NOvA+), T2HK, a WBB with a baseline of 2300 km and a 100 kton LAr detector (WBB), a low energy betabeam combined with the SPL superbeam and aimed at WC detector at 130 km, a higher energy betabeam (BB350), a neutrino factory with 10 GeV (NF10) and 5 GeV (NF5) muons and a 100 kton MIND detector, as well as the expected reach by 2020 by combining NOvA, T2K, and reactor data. Figure is taken from [149].

for the low detection cross-section and excellent sensitivity to CP violation can be reached; see Figure 15. CP violation can be found at 3σ for ~67% of the values of δ for $\sin^2\theta_{13} = 0.1$ [68] (see also [113]). Due to the short distance, no matter effects arise and no sensitivity to the mass hierarchy can be achieved from long baseline neutrino oscillations. However, given the recently discovered large value of θ_{13}, taking into account atmospheric neutrino events will allow to find the hierarchy for sufficient exposure; see Figure 6 [68].

5.2. Betabeams. Betabeams [114–116] have been proposed as an alternative type of setup which uses a very pure beam of electron neutrinos produced by beta-decays of highly accelerated ions. In this case, the main oscillation channel is the $\nu_e \rightarrow \nu_\mu$, one which provides sensitivity to the mass hierarchy and CP violation. The neutrino spectrum is very well known and depends on the Q value of the beta-decay and on the γ factor of the ions. In a given accelerator, for example, the Main Injector at Fermilab or the SPS at CERN, fully stripped ions can be accelerated to a maximum Z/A times the proton energy, with Z and A the number of protons and of nucleons, respectively. After the initial idea, subsequent studies were performed in the context of EURISOL and EUROnu Design Studies. The ions, which have suitable lifetimes and can be copiously produced, are the combinations: ^{6}He, ^{18}Ne, and ^{8}Li, ^{8}B, for ν_e and $\overline{\nu}_e$ beams. The former has Q values of 3.5 MeV and 3.3 MeV, respectively, while ^{8}Li, ^{8}B of 13.0 MeV and 13.9 MeV, respectively. The latter ions will yield higher neutrino energies for a given γ, but the flux will be lower for the same energy as it scales as γ^{-2}. All of these isotopes need to be produced artificially, and the production rate turns out to be a limiting factor for the physics reach of the facilities. ^{6}He, ^{18}Ne pose less-significant challenges from the production point of view but do not allow to reach very high energies, while the other ions could provide higher energies without the need for high γ-factors, but, due to the challenges of production, it is still not clear what fluxes could be achievable.

The $\gamma = 100$ option for a betabeam which uses ^{6}He, ^{18}Ne has been studied in detail within the EURISOL Design Study. Given the very low energies, the most suitable baseline is the CERN to Fréjus one of 130 km. In principle, higher γ factors could be achieved if a significant upgrade of the present accelerators is envisaged [117]; see also [70, 118–125]. In this case, higher energies and consequently longer distances could be used which provide sensitivity not only to CP violation but also to matter effects. The ideal detector, given the low energies of the beam, is MEMPHYS, a one megaton Water-Cerenkov detector, which has excellent energy resolution and efficiency. Compared to superbeams, betabeams have an extremely pure beam, with no contamination from other flavours at the source. On the other hand, the absence of a ν_μ component implies that a betabeam cannot provide a precision measurement of θ_{23}. Due to the short distance, no sensitivity to the mass hierarchy is achievable, as in the case of the SPL, unless atmospheric neutrinos are included [68]. Excellent reach for CP violation could be obtained, especially if the betabeam is combined with a superbeam from CERN to Fréjus. The two setups are sensitive to the T-conjugated channels, providing a clean measurement of the CP-violating phase δ; see Figure 15. Moreover the betabeam-superbeam combination offers also improved sensitivity to the mass hierarchy, even in the case of short baselines [69]; see Figure 6.

5.3. Neutrino Factory. In a Neutrino Factory [126–128] neutrinos are produced by highly accelerated muons which decay producing a highly collimated beam of muon and electron neutrinos. The spectrum is very well known and high energies can be achieved: the wide beam and high energies allow to reconstruct with precision the oscillatory pattern and typically achieve a superior performance with respect to the other options. Let us consider the decay of μ^- (μ^+): it will generate an initial beam with two neutrino components, ν_μ and $\overline{\nu}_e$ ($\overline{\nu}_\mu$ and ν_e). These will oscillate inducing also ν_e and $\overline{\nu}_\mu$ ($\overline{\nu}_e$ and ν_μ). At the detector, for muon-like events, two different signals will be present: the *right-sign* muon events which derive from the observation of ν_μ coming from the disappearance channel, $\nu_\mu \rightarrow \nu_\mu$, and the *wrong-sign* muon events which are due to $\overline{\nu}_e \rightarrow \overline{\nu}_\mu$ oscillations. As the appearance oscillation is sensitive to matter effects and CPV, it is necessary to distinguish the two signals. This is achieved by means of magnetized detectors which can distinguish μ^+ from μ^- events. The mis-Id rate is typically very low at a

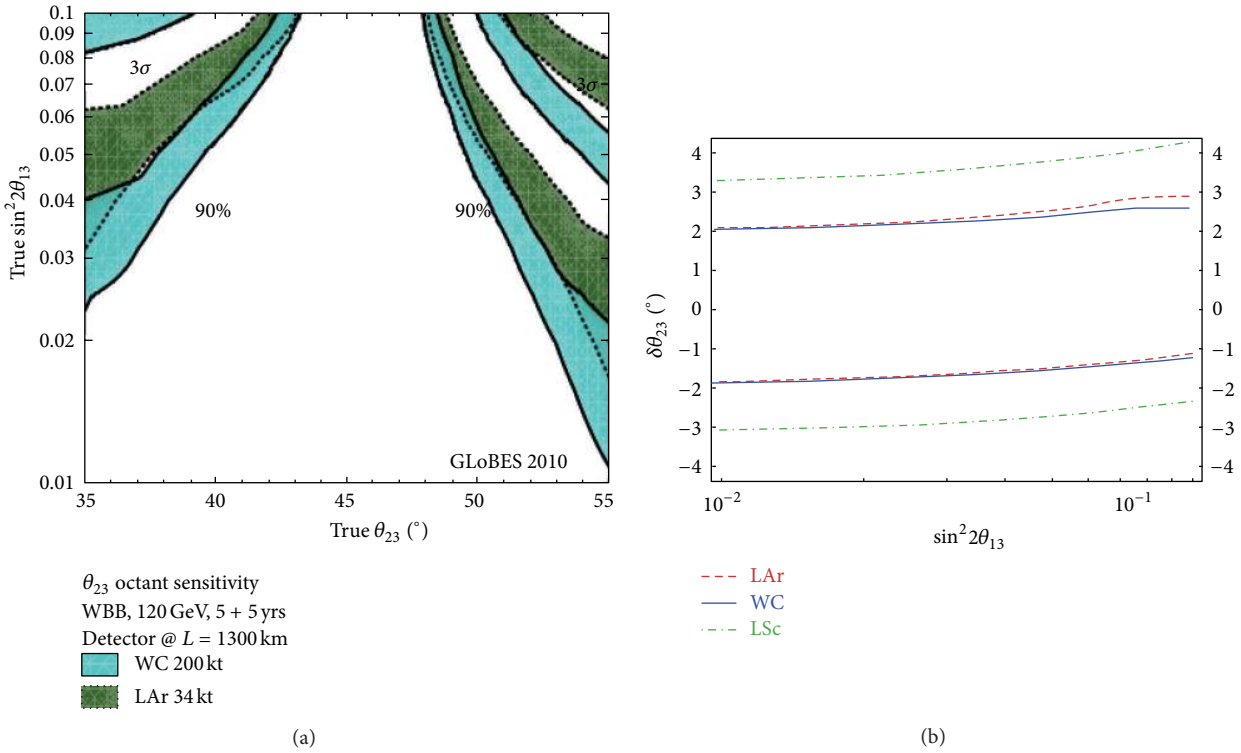

FIGURE 20: (a) LBNE sensitivity to resolve the θ_{23} octant degeneracy. The standard configuration in 2010 has been used. The blue (green) band shows the results for 200 kt WC (34 kt LAr) and its width is obtained by varying δ, ranging from 10% to 90% CP fraction. In the region above the bands, the θ_{23} octant can be determined at 90% CL (lower bands) and 3σ (upper bands). Taken from [103]. (b) Nonmaximal θ_{23} discovery potential, with $\delta\theta_{23} \equiv \theta_{23} - 45^\circ$, as a function of $\sin^2 2\theta_{13}$, for the LBNO superbeam with 100 kton LAr, 440 kton WC and 50 kton LSc detectors. In the region enclosed by each couple of lines, $\delta\theta_{23} = 0$ cannot be ruled out at a statistical significance of 3σ. Results are shown for the detector placed at Pyhäsalmi and for a true normal hierarchy. Figure taken from [107].

level of 10^{-4}–10^{-3}, depending on the detector technology. The detector of choice [129] is an iron-magnetized detector (MIND) which provides excellent background rejection and very good energy resolution but low detection efficiency for neutrinos with energies in the few GeV range. This detector performs very well for high energies and is the default choice for muon energies above 8 GeV. For lower energies, detectors with lower-Z would be preferred, such as a magnetized Totally-Active Scintillator Detector (TASD) or LAr. The latter detectors provide excellent efficiency for neutrinos with low energies, excellent energy resolution, and low backgrounds, but their magnetization is extremely challenging and not proven yet for the mass scales of interest. (In [130] the possibility to use nonmagnetized detectors for a neutrino factory has been put forward, which may become an option for large θ_{13} and offers an interesting synergy with large-scale detectors for nonaccelerator physics. More detailed studies along these lines would be required, and this option is currently not considered within the context of neutrino factory study groups.)

The initial baseline configuration of the NF [129] used muons with an energy of 25 GeV and two different baselines, at approximately 4000 and 7500 km, with two MIND detectors, a 100 kton one at the shorter baseline and a 50 kton one at the "magic" baseline [131]. This second baseline was designed to provide a very powerful determination of the mass hierarchy and a clean determination of θ_{13}, thanks to the strong suppression of the "CP term" due to $\sin \Delta A \sim 0$, and to complement the shorter baseline in the search of CP violation, helping to resolve the degeneracies. Additional studies can be found, for example, in [84, 132–141]. This setup was optimised assuming small values of θ_{13}, and several studies showed that it would outperform all other options for small θ_{13}, thanks to its high number events, very low backgrounds, and small systematic errors [129, 140].

In the case of large θ_{13}, a more conservative setup, named the Low-Energy Neutrino Factory (LENF), was proposed as a less-challenging option [142, 143] which used a single baseline of 1300 km, corresponding to the Fermilab to DUSEL distance, and, consequently, a lower muon energy, at ~4.5 GeV [144]; see also [145, 146]. Given the low energy, a detector with good-energy resolution and low-energy threshold was needed in order to exploit the rich oscillatory pattern. The detector of choice was a Totally-Active Scintillator Detector (TASD) magnetized by means of a large magnetic cavern or a magnetized LAr TPC, which would be ideal due to the large size and the excellent detector performance, especially at low energy. This initial study showed that excellent reach could be

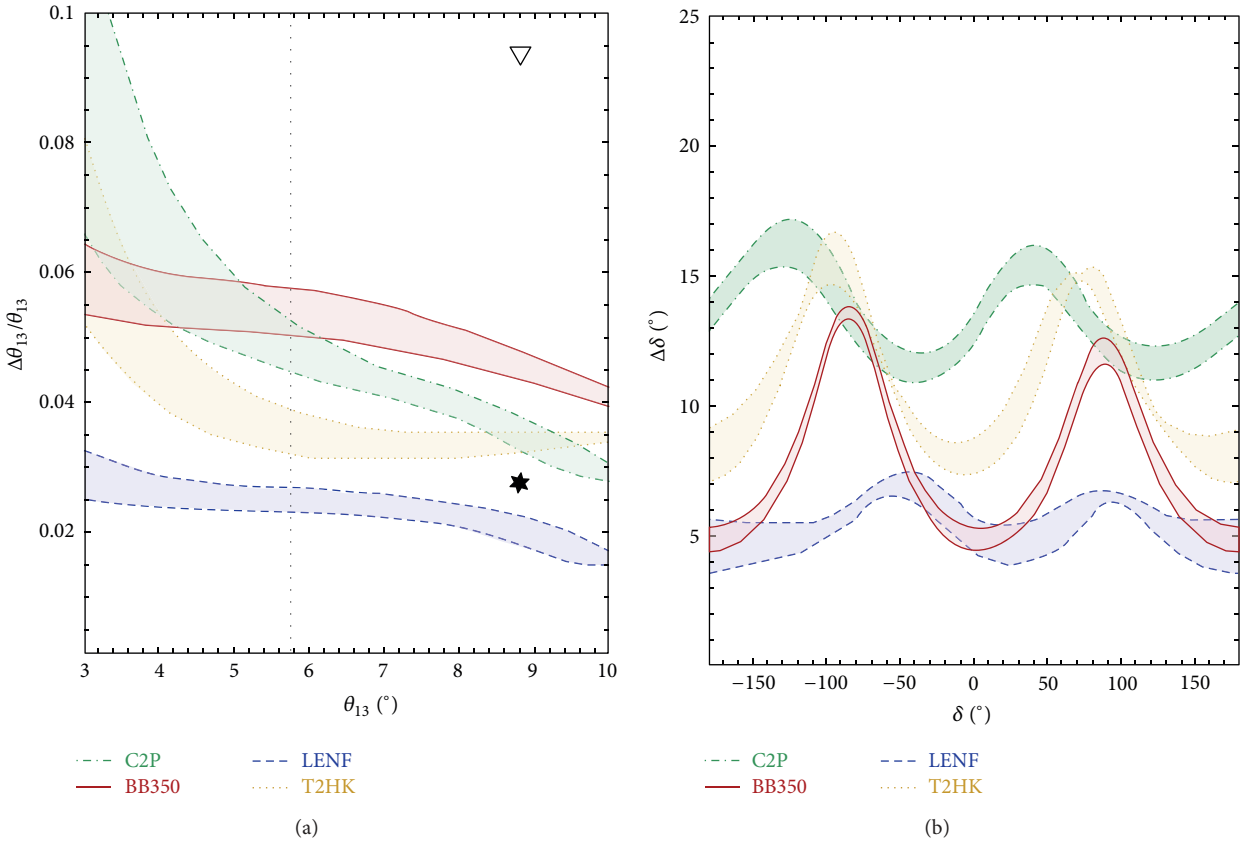

FIGURE 21: 1σ precision on θ_{13} (a) and δ (b) for the CN2PY and T2HK superbeams, the $\gamma = 350$ beta-beam, and the LENF. On the left plot, the empty triangle represents the current precision for Daya Bay, and the star the ultimate attainable precision, assuming as true value the present Daya Bay best fit value. The width of the bands represent the dependence of the error on θ_{13} on δ and vice versa. For further details, see [46] from which the figure is reproduced.

achieved for the mass hierarchy and CP violation; see Figure 16. A subsequent study of the LENF using a Magnetized Iron Neutrino Detector has also shown a promising performance [147], and its reach is reported in Figure 17. A similar study using a TASD and LAr detector [148] found a rather flat performance as a function of L and muon energy, for large θ_{13}, as seen in Figure 18. Based on these analyses and in view of the discovery of large θ_{13}, the International Design Study on a Neutrino Factory (IDS-NF) reviewed the baseline configuration in April 2012 and chose a LENF with MIND detector with muon energy of 10 GeV and baseline of 2000 km.

A summary of the results for the LENF and a comparison with other facilities are given in Figure 19 [149]. A table which summarises the setups described and their reach for CP violation is given in Table 4. A word of caution is necessary as the precise reach of each setup is affected by the assumption made on the beam, detector, and systematic errors. Nevertheless, thanks to the intense flux, pure beam, excellent background rejection, and long baselines, an NF has been shown to achieve the best physics reach in search for CP violation and the mass hierarchy.

Once CP violation is discovered, it will be important to measure the values of the phase and of θ_{13} with high precision. In fact, in many models of leptonic flavour, these values are correlated with the deviations from maximality of θ_{23} and/or with parameters in the quark sector. Examples of the precision achievable have been typically included in the analysis of the setups, but a comprehensive and detailed study is still at its beginnings. A first comparison between different experiments has been performed in [46]. The main results are reported in Figure 21 and indicate that for θ_{13} reactor experiments, and in particular Daya Bay, will achieve the best precision, marginally improved by a LENF. The precise measurement of the δ phase depends significantly on the true value itself, with a significant loss of precision around $\pi/2$ for experiments such as T2HK and beta beams. If instead matter effects are relevant, as it is the case for CN2PY and LENF, the error on δ tends to become more uniform in δ, and the best performance is given by the LENF which can typically achieve an error of around 5°.

5.4. Precision Measurements. With the discovery of large θ_{13}, the focus of future long baseline experiments has shifted not only to the discovery of the mass hierarchy and CP violation as discussed above but also to the precise measurements of the oscillation parameters. Among these, determining if θ_{23} is maximal or not is of great theoretical importance together with establishing its octant, if nonmaximal. The experiments discussed in the previous subsections, except beta beams, will have sensitivity to these parameters mainly

Table 4: Summary of the setups described in the text. From left to right, the columns list the names of the setups, the beam power for superbeams or γ factor for beta beams or muon energy for neutrino factories, the baseline, the detector choice, the running time in years for each polarity (the neutrino and antineutrinos runs are simultaneous for the neutrino factory), the systematic error on the signal and background, the fraction of the values of δ for which CP-violation could be determined at 3σ at $\sin^2 2\theta_{13} = 0.1$, and the reference from which the information has been collected. For LBNO with 10 kton and 30 kton LAr detectors, the values of the fraction of δ are given separately for a true normal (NH) or inverted (IH) hierarchy. The number of seconds per year is 1.7×10^7 for LBNO and 1×10^7 for T2HK. BB + SPL considers the combination of the betabeam with 1.1×10^{18} (2.8×10^{18}) ^{18}Ne (^{6}He) useful decays per year together with the SPL described above (with a 500 kton WC detector instead of a 440 kton one). The LENF uses 1.4×10^{21} useful muon decays per year per polarity, and NF10 7×10^{20}. The results quoted depend significantly on the assumptions made in the analysis and should be treated carefully.

Setup	MW	L	Detector	Years $\nu + \overline{\nu}$	Syst. errors (signal, backg.)	3σ CPV reach	References
LBNE	0.7	1290 km	200 kton WC or 34 kton LAr	5 + 5	(1%, 5%)	~60%	[103]
LBNE12	0.7	1290 km	10 kton LAr	5 + 5	(1%, 5%)	27%	[104]
LBNO	4	130 km	440 kton WC	2 + 8	(5%, 5%)	~60%	[107]
	1.6	2290 km	10 kton LAr	5 + 5	(5%, 5%)	25% (NH)–38% (IH)	[112]
	1.6	2290 km	30 kton LAr	5 + 5	(5%, 5%)	58% (NH)–62% (IH)	[112]
	1.6	2290 km	100 kton LAr	5 + 5	(5%, 5%)	71%	[112]
T2HK	1.66	295	560 kton WC	1.5 + 3.5	~(5%, 5%)	75%	[66]
	1.66	295	560 kton WC	1.5 + 3.5	~(5%, 5%)	55% no mass hier.	[66]
SPL	4	130 km	440 kton WC	2 + 8	(2%, 2%)	73%	[68]
	4	130 km	440 kton WC	2 + 8	(5%, 5%)	53%	[68]
	γ						
BB + SPL	100	130	500 kton WC	5 + 5	See [149]	80%	[149]
BB350	350	650	500 kton WC	5 + 5	See [149]	~70%	[149]
	E_μ						
LENF	4.5 GeV	1300 km	20 kton TASD 100 kton LAr	10	(2%, 2%)	85% 81%–90%	[144]
NF10	10 GeV	2000 km	100 kton MIND	10	(2%, 2%)	86%	[149]

via the disappearance channels $\nu_\mu \to \nu_\mu$ and $\overline{\nu}_\mu \to \overline{\nu}_\mu$. Typically superbeams have a very good reach and a LENF can perform better especially if the low energy part of the spectrum can be reconstructed. It has been shown that the contamination from ν_τ events, coming from $\nu_\mu \to \nu_\tau$ oscillations, can have a significant impact on the high energy neutrino factory [150, 151]. It is expected that a lower muon energy will reduce the number of τ events but their impact in the 10 GeV LENF needs to be fully explored. In Figure 20 we report two examples of the capability of LBNE in the 2010 configuration and of the 4.5 GeV LENF for studying θ_{23}.

6. Conclusions

Since the discovery of neutrino oscillations huge progress has been made and this phenomenon is now well established. Yet new important questions are open for the future, including what is the ordering of neutrino masses? Is there CP violation in the leptonic sector? What are the precise values of the neutrino mixing parameters? Are there new phenomena beyond the three-neutrino framework? With the recently discovered relatively large value of the mixing angle θ_{13}, addressing those questions by upcoming oscillation experiments becomes a realistic possibility. In this paper, we have reviewed the phenomenology of oscillation experiments by discussing some aspects of the determination of neutrino oscillation parameters by present global data, and we have tried to give an outlook for possible future developments. In the near term (the next 10 to 15 years), the interplay of complementary data sets will be important, such as long-baseline accelerator experiments, reactor experiments, and atmospheric neutrino experiments. We have discussed the potential to address questions like the nonmaximality and the octant of θ_{23} and the determination of the neutrino mass hierarchy. In order to address CP violation, it seems from the current perspective that a more long-term program will be necessary. Future high-precision long-baseline neutrino experiments can provide crucial answers to the above questions by studying the subdominant $\nu_\mu \to \nu_e$ transitions. A wide experimental program for the future is underway or at the discussion stage and includes superbeams, betabeams and neutrino factory. A table which summarises various setups and their reach for CP violation is given in Table 4.

Acknowledgment

The authors acknowledge partial support from the European Union FP7 ITN INVISIBLES (Marie Curie Actions, PITN-GA-2011-289442).

References

[1] Y. Fukuda, T. Hayakawa, E. Ichihara et al., "Evidence for oscillation of atmospheric neutrinos," *Physical Review Letters*, vol. 81, no. 8, pp. 1562–1567, 1998.

[2] Q. R. Ahmad, R. C. Allen, T. C. Andersen et al., "Direct evidence for neutrino avor transformation from neutral current interactions in the sudbury neutrino observatory," *Physical Review Letters*, vol. 89, no. 1, Article ID 011301, 6 pages, 2002.

[3] T. Araki, K. Eguchi, S. Enomoto et al., "Measurement of neutrino oscillation with KamLAND: evidence of spectral distortion," *Physical Review Letters*, vol. 94, no. 8, Article ID 081801, 2005.

[4] P. Adamson, C. Andreopoulos, K. E. Arms et al., "Measurement of neutrino oscillations with the MINOS detectors in the NuMI beam," *Physical Review Letters*, vol. 101, no. 13, Article ID 131802, 5 pages, 2008.

[5] K. Abe, N. Abgrall, Y. Ajima et al., "Indication of electron neutrino appearance from an accelerator-produced off-axis muon neutrino beam," *Physical Review Letters*, vol. 107, no. 4, Article ID 041801, 2011.

[6] P. Adamson, MINOS Collaboration et al., "Improved search for muon-neutrino to electronneutrino oscillations in MINOS," *Physical Review Letters*, vol. 107, no. 18, Article ID 181802, 6 pages, 2011.

[7] Y. Abe, C. Aberle, T. Akiri et al., "Indication for the disappearance of reactor electron antineutrinos in the Double Chooz experiment," *Physical Review Letters*, vol. 108, Article ID 131801, 7 pages, 2012.

[8] F. An, J. Z. Bai, A. B. Balantekin et al., "Observation of electron-antineutrino disappearance at Daya Bay," *Physical Review Letters*, vol. 108, no. 17, Article ID 171803, 7 pages, 2012.

[9] J. Ahn, S. Chebotaryov, J. H. Choi et al., "Observation of reactor electron antineutrino disappearance in the RENO experiment," *Physical Review Letters*, vol. 108, no. 19, Article ID 191802, 6 pages, 2012.

[10] M. C. Gonzalez-Garcia, M. Maltoni, J. Salvado, and T. Schwetz, "Global fit to three neutrino mixing: critical look at present precision," *Journal of High Energy Physics*, vol. 2012, article 123, 2012.

[11] D. Forero, M. Tortola, and J. Valle, "Global status of neutrino oscillation parameters after recent reactor measurements," *Physical Review D*, vol. 86, Article ID 073012, 8 pages, 2012.

[12] G. Fogli, E. Lisi, A. Marrone et al., "Global analysis of neutrino masses, mixings and phases: entering the era of leptonic CP violation searches," *Physical Review D*, vol. 86, no. 1, Article ID 013012, 10 pages, 2012.

[13] P. Machado, H. Minakata, H. Nunokawa, and R. Z. Funchal, "Combining accelerator and reactor measurements of θ_{13} the first result," *Journal of High Energy Physics*, vol. 1205, article 023, 2012.

[14] J. Bergstrom, "Bayesian evidence for non-zero θ_{13} and CP-violation in neutrino oscillations," *Journal of High Energy Physics*, vol. 2012, article 163, 2012.

[15] G. Mention, M. Fechner, Th. Lasserre et al., "The reactor antineutrino anomaly," *Physical Review D*, vol. 83, no. 7, Article ID 073006, 2011.

[16] M. Apollonio, A. Baldini, C. Bemporad et al., "Search for neutrino oscillations on a long base-line at the CHOOZ nuclear power station," *The European Physical Journal*, vol. C27, Article ID 030101, p. 331, 2003.

[17] J. Beringer, J. F. Arguin, R. M. Barnett et al., "Review of particle physics," *Physical Review D* , vol. 86, no. 1, Article ID 010001, 1528 pages, 2012.

[18] H. Minakata, H. Sugiyama, O. Yasuda, K. Inoue, and F. Suekane, "Reactor measurement of θ_{13} and its complementarity to long baseline experiments," *Physical Review D*, vol. 68, Article ID 033017, 21 pages, 2003.

[19] P. Huber, M. Lindner, T. Schwetz, and W. Winter, "Reactor neutrino experiments compared to superbeams," *Nuclear Physics B*, vol. 665, pp. 487–519, 2003.

[20] G. L. Fogli and E. Lisi, "Tests of three-flavor mixing in long-baseline neutrino oscillation experiments," *Physical Review D*, vol. 54, no. 5, pp. 3667–3670, 1996.

[21] R. Nichols, "Results from MINOS," Talk at Neutrino 2012, Kyoto, Japan, June 2012.

[22] K. B. M. Mahn and M. H. Shaevitz, "Comparisons and combinations of reactor and long-baseline neutrino oscillation measurements," *International Journal of Modern Physics A*, vol. 21, no. 18, pp. 3825–3843, 2006.

[23] A. Cervera, A. Donini, M. B. Gavela, J. J. Gomez Cádenas, P. Hernández, and O. Mena, "Golden measurements at a neutrino factory," *Nuclear Physics*, vol. 579, no. 1, Article ID 000210, pp. 17–55, 2000.

[24] M. Freund, "Analytic approximations for three neutrino oscillation parameters and probabilities in matter," *Physical Review*, vol. 64, no. 5, Article ID 053003, 12 pages, 2001.

[25] E. K. Akhmedov, R. Johansson, M. Lindner et al., "Series expansions for three avor neutrino oscillation probabilities in matter," *Journal of High Energy Physics*, vol. 0404, article 078, Article ID 040217, 2004.

[26] L. Wolfenstein, "Neutrino oscillations in matter," *Physical Review D*, vol. 17, no. 9, pp. 2369–2374, 1978.

[27] S. Mikheev and A. Y. Smirnov, "Resonance amplification of oscillations in matter and spectroscopy of solar neutrinos," *Soviet Journal of Nuclear Physics*, vol. 42, article 913, 1985.

[28] D. Ayres and NOvA Collaboration, "NOvA: proposal to build a 30 kiloton off-axis detector to study $\upsilon_u \rightarrow \upsilon_e$ oscillations in the NuMI beamline," In press, http://arxiv.org/abs/hep-ex/0503053.

[29] V. Barger, D. Marfatia, and K. Whisnant, "Breaking eight-fold degeneracies in neutrino CP violation, mixing, and mass hierarchy," *Physical Review D*, vol. 65, Article ID 073023, 2002.

[30] O. L. G. Peres and A. Y. Smirnov, "Atmospheric neutrinos: LMA oscillations, Ue3 induced interference and CP-violation," *Nuclear Physics B*, vol. 680, no. 1–3, pp. 479–509, 2004.

[31] S. T. Petcov, "Diffractive-like (or parametric-resonance-like?) enhancement of the Earth (day-night) effect for solar neutrinos crossing the Earth core," *Physics Letters B*, vol. 434, no. 3-4, pp. 321–332, 1998.

[32] E. K. Akhmedov, "Parametric resonance of neutrino oscillations and passage of solar and atmospheric neutrinos through the earth," *Nuclear Physics B*, vol. 538, no. 1-2, pp. 25–51, 1999.

[33] E. K. Akhmedov, A. Dighe, P. Lipari, and A. Y. Smirnov, "Atmospheric neutrinos at super-Kamiokande and parametric resonance in neutrino oscillations," *Nuclear Physics B*, vol. 542, no. 1-2, pp. 3–30, 1999.

[34] M. Chizhov, M. Maris, and S. T. Petcov, "On the oscillation length resonance in the transitions of solar and atmospheric neutrinos crossing the earth core," In press, http://arxiv.org/abs/hep-ph/9810501.

[35] M. V. Chizhov and S. T. Petcov, "New conditions for a total neutrino conversion in a medium," *Physical Review Letters*, vol. 83, no. 6, pp. 1096–1099, 1999.

[36] E. K. Akhmedov, M. Maltoni, and A. Y. Smirnov, "1–3 leptonic mixing and the neutrino oscillograms of the Earth," *Journal of High Energy Physics*, vol. 0705, article 077, Article ID 061228, 2007.

[37] C. W. Kim and U. W. Lee, "Comment on the possible electron neutrino excess in the Super-Kamiokande atmospheric neutrino experiment," *Physics Letters B*, vol. 444, no. 1-2, pp. 204–207, 1998.

[38] O. Peres and A. Y. Smirnov, "Testing the solar neutrino conversion with atmospheric neutrinos," *Physics Letters B*, vol. 456, article 204, Article ID 990231, 1999.

[39] M. Gonzalez-Garcia, M. Maltoni, and A. Y. Smirnov, "Measuring the deviation of the 2-3 lepton mixing from maximal with atmospheric neutrinos," *Physical Review D*, vol. 70, Article ID 093005, 2004.

[40] E. K. Akhmedov, M. Maltoni, and A. Y. Smirnov, "Neutrino oscillograms of the Earth: effects of 1-2 mixing and CP-violation," *Journal of High Energy Physics*, vol. 0806, article 072, 2008.

[41] J. Bernabéu, S. Palomares-Ruiz, and S. T. Petcov, "Atmospheric neutrino oscillations, θ_{13} and neutrino mass hierarchy," *Nuclear Physics B*, vol. 669, no. 1-2, pp. 255–276, 2003.

[42] S. T. Petcov and T. Schwetz, "Determining the neutrino mass hierarchy with atmospheric neutrinos," *Nuclear Physics B*, vol. 740, no. 1-2, pp. 1–22, 2006.

[43] Y. Itow, "Results from running experiments," Talk at Neutrino 2012, Kyoto, Japan, 2012.

[44] M. Mezzetto and T. Schwetz, "θ_{13} Phenomenology, present status and prospect," *Journal of Physics G*, vol. 37, no. 10, Article ID 103001, 2010.

[45] P. Huber, M. Lindner, T. Schwetz, and W. Winter, "First hint for CP violation in neutrino oscillations from upcoming superbeam and reactor experiments," *Journal of High Energy Physics*, vol. 2009, no. 11, 2009.

[46] P. Coloma, A. Donini, E. Fernandez-Martinez, and P. Hernandez, "Precision on leptonic mixing parameters at future neutrino oscillation experiments," *Journal of High Energy Physics*, vol. 1206, article 073, 2012.

[47] H. Minakata and H. Nunokawa, "Exploring neutrino mixing with low energy superbeams," *Journal of High Energy Physics*, vol. 5, no. 10, 2001.

[48] S. Prakash, S. K. Raut, and S. U. Sankar, "Getting the best out of T2K and NOνA," *Physical Review D*, vol. 86, no. 3, Article ID 033012, 2012.

[49] A. S. Dighe and A. Y. Smirnov, "Identifying the neutrino mass spectrum from a supernova neutrino burst," *Physical Review D*, vol. 62, no. 3, Article ID 033007, pp. 1–24, 2000.

[50] M. Kachelriess, R. Tomas, R. Buras et al., "Exploiting the neutronization burst of a galactic supernova," *Physical Review D*, vol. 71, Article ID 063003, 2005.

[51] P. D. Serpico, S. Chakraborty, T. Fischer et al., "Probing the neutrino mass hierarchy with the rise time of a supernova burst," *Physical Review D*, vol. 85, Article ID 085031, 2012.

[52] E. Borriello, S. Chakraborty, A. Mirizzi et al., "(Down-to-)Earth matter effect in supernova neutrinos," *Physical Review D*, vol. 86, Article ID 083004, 2012.

[53] S. Pascoli, S. T. Petcov, and T. Schwetz, "The absolute neutrino mass scale, neutrino mass spectrum, Majorana CP-violation and neutrinoless double-beta decay," *Nuclear Physics B*, vol. 734, no. 1-2, pp. 24–49, 2006.

[54] W. Rodjohann, "Neutrino-less double beta decay and particle physics," *International Journal of Modern Physics E*, vol. 20, article 1833, 2011.

[55] N. Mondal, "India-based neutrino observatory," Talk at Lepton-Photon 2011, TIFR, Mumbai, India, 2011, http://www.tifr.res.in/~lp11/.

[56] "India-Based Neutrino Observatory," http://www.ino.tifr.res.in/ino/.

[57] R. Gandhi, P. Ghoshal, S. Goswami, and S. U. Sankar, "Resolving the mass hierarchy with atmospheric neutrinos using a liquid argon detector," *Physical Review D*, vol. 78, no. 7, Article ID 073001, 2008.

[58] V. Barger, R. Gandhi, P. Ghoshal et al., "Neutrino mass hierarchy and octant determination with atmospheric neutrinos," vol. 109, Article ID 091801, 2012.

[59] T. T. de Fatis, "Prospects of measuring $\sin^2 2\Theta_{13}$ and the sign of Δm^2 with a massive magnetized detector for atmospheric neutrinos," *The European Physical Journal C*, vol. 24, no. 1, pp. 43–50, 2000.

[60] M. Blennow and T. Schwetz, "Identifying the neutrino mass ordering with INO and NOvA," *Journal of High Energy Physics*, vol. 2012, no. 8, article 058, 2012.

[61] M. Blennow and T. Schwetz, "Erratum: Identifying the neutrino mass ordering with INO and NOvA (Journal of High Energy Physics (2012) 08 (058))," *Journal of High Energy Physics*, vol. 2012, no. 11, article 098, 2012.

[62] R. Gandhi, P. Ghoshal, S. Goswami, P. Mehta, S. U. Sankar, and S. Shalgar, "Mass hierarchy determination via future atmospheric neutrino detectors," *Physical Review D*, vol. 76, no. 7, Article ID 073012, 20 pages, 2007.

[63] A. Samanta, "A comparison of the ways of resolving mass hierarchy with atmospheric neutrinos," *Physical Review D*, vol. 81, no. 3, Article ID 037302, 4 pages, 2010.

[64] D. Indumathi and M. Murthy, "A qestion of hierarchy: matter effects with atmospheric neutrinos and anti-neutrinos," *Physical Review D*, vol. 71, no. 1, Article ID 013001, 16 pages, 2005.

[65] D. Autiero, J. Aysto, A. Badertscher et al., "Large underground, liquid based detectors for astro-particle physics in Europe: scientific case and prospects," *Journal of Cosmology and Astroparticle Physics*, vol. 2007, article 011, 2007.

[66] K. Abe, T. Abe, H. Aihara et al., "Letter of intent: the Hyper-Kamiokande experiment—detector design and physics potential," In press, http://arxiv.org/abs/1109.3262.

[67] P. Huber, M. Maltoni, and T. Schwetz, "Resolving parameter degeneracies in long-baseline experiments by atmospheric neutrino data," *Physical Review D*, vol. 71, no. 5, Article ID 053006, 15 pages, 2005.

[68] J.-E. Campagne, M. Maltoni, M. Mezzetto, and T. Schwetz, "Physics potential of the CERN-MEMPHYS neutrino oscillation project," *Journal of High Energy Physics*, vol. 2007, article 003, 2007.

[69] T. Schwetz, "Determination of the neutrino mass hierarchy in the regime of small matter effect," *Journal of High Energy Physics*, vol. 2007, article 093, Article ID 070327, 2007.

[70] A. Jansson, O. Mena, S. J. Parke, and N. Saoulidou, "Combining CPT-conjugate neutrino channels at Fermilab," *Physical Review D*, vol. 78, no. 5, Article ID 053002, 11 pages, 2008.

[71] M. C. Gonzalez-Garcia, F. Halzen, and M. Maltoni, "Physics reach of high-energy and high-statistics IceCube atmospheric neutrino data," *Physical Review D*, vol. 71, no. 9, Article ID 093010, 13 pages, 2005.

[72] R. Abbasi, Y. Abdou, M. Ackermann et al., "The design and performance of IceCube DeepCore," *Astroparticle Physics*, vol. 35, no. 10, pp. 615–624, 2012.

[73] The IceCube Collaboration, "Atmospheric neutrino oscillations with IceCube/DeepCore," in *Proceedings of the International Conference on Neutrino Physics and Astrophysics (ICNPA '12)*, Kyoto, Japan, June 2012.

[74] O. Mena, I. Mocioiu, and S. Razzaque, "Neutrino mass hierarchy extraction using atmospheric neutrinos in ice," *Physical Review D*, vol. 78, no. 9, Article ID 093003, 10 pages, 2008.

[75] D. J. Koskinen, "IceCube-DeepCore-PINGU: fundamental neutrino and dark matter physics at the South Pole," *Modern Physics Letters A*, vol. 26, no. 39, pp. 2899–2915, 2011.

[76] E. K. Akhmedov, S. Razzaque, and A. Y. Smirnov, "Mass hierarchy, 2-3 mixing and CP-phase with huge atmospheric neutrino detectors," In press, http://arxiv.org/abs/1205.7071.

[77] S. T. Petcov and M. Piai, "The LMA MSW solution of the solar neutrino problem, inverted neutrino mass hierarchy and reactor neutrino experiments," *Physics Letters B*, vol. 533, no. 1-2, pp. 94–106, 2002.

[78] J. G. Learned, S. T. Dye, S. Pakvasa, and R. C. Svoboda, "Determination of neutrino mass hierarchy and θ_{13} with a remote detector of reactor antineutrinos," *Physical Review D*, vol. 78, no. 7, Article ID 071302, 5 pages, 2008.

[79] L. Zhan, Y. Wang, J. Cao, and L. Wen, "Experimental requirements to determine the neutrino mass hierarchy using reactor neutrinos," *Physical Review D*, vol. 79, no. 7, Article ID 073007, 5 pages, 2009.

[80] P. Ghoshal and S. Petcov, "Neutrino mass hierarchy determination using reactor antineutrinos," *Journal of High Energy Physics*, vol. 2011, article 58, 2011.

[81] J. Cao, "Observation of electron antineutrino disappearance at Daya Bay," in *Proceedings of the Neutrino at the Turning Point (nu-TURN '12)*, Laboratori Nazionali del Gran Sasso, Assergi, Italy, May 2012.

[82] S. T. Petcov and T. Schwetz, "Precision measurement of solar neutrino oscillation parameters by a long-baseline reactor neutrino experiment in Europe," *Physics Letters B*, vol. 642, no. 5-6, pp. 487–494, 2006.

[83] J. Alonso, F. T. Avignone, W. A. Barletta et al., "Expression of interest for a novel search for CP violation in the neutrino sector: DAEdALUS," In press, http://arxiv.org/abs/1006.0260.

[84] J. B. Castell, M. B. Gavela, J. J. Cadenas, P. Hernández, and O. Mena, "On the measurement of leptonic CP violation," *Nuclear Physics B*, vol. 608, no. 1-2, pp. 301–318, 2001.

[85] H. Minakata, H. Nunokawa, and S. J. Parke, "Parameter degeneracies in neutrino oscillation measurement of leptonic CP and *T* violation," *Physical Review D*, vol. 66, no. 9, Article ID 093012, 15 pages, 2002.

[86] V. D. Barger, S. Geer, R. Raja, and K. Whisnant, "Exploring neutrino oscillations with superbeams," *Physical Review D*, vol. 63, no. 11, Article ID 113011, 24 pages, 2001.

[87] T. Kajita, H. Minakata, and H. Nunokawa, "Method for determination of $|U_{e3}|$ in neutrino oscillation appearance experiments," *Physics Letters B*, vol. 528, no. 3-4, pp. 245–252, 2002.

[88] H. Minakata, H. Nunokawa, and S. Parke, "Parameter degeneracies in neutrino oscillation measurement of Ieptonic CP and T violation," *Physical Review D*, vol. 66, no. 9, Article ID 093012, 2002.

[89] H. Minakata and H. Nunokawa, "How to measure CP violation in neutrino oscillation experiments?" *Physics Letters B*, vol. 413, no. 3-4, pp. 369–377, 1997.

[90] V. Barger, D. Marfatia, and K. Whisnant, "Off-axis beams and detector clusters: resolving neutrino parameter degeneracies," *Physical Review D*, vol. 66, no. 5, Article ID 053007, 2002.

[91] O. M. Requejo, S. Palomares-Ruiz, and S. Pascoli, "Super-NOνA: a long-baseline neutrino experiment with two off-axis detectors," *Physical Review D*, vol. 72, no. 5, Article ID 053002, 2005.

[92] O. Mena, S. Palomares-Ruiz, and S. Pascoli, "Determining the neutrino mass hierarchy and CP-violation in NOνA with a second off-axis detector," *Physical Review D*, vol. 73, no. 7, Article ID 073007, 2006.

[93] J. Bernabeu, J. Burguet-Castell, C. Espinoza, and M. Lindroos, "Monochromatic neutrino beams," *Journal of High Energy Physics*, no. 12, pp. 271–279, 2005.

[94] M. Ishitsuka, T. Kajita, H. Minakata, and H. Nunokawa, "Resolving the neutrino mass hierarchy and CP degeneracy by two identical detectors with different baselines," *Physical Review D*, vol. 72, no. 3, Article ID 033003, pp. 1–14, 2005.

[95] K. Hagiwara, N. Okamura, and K. Senda, "Solving the neutrino parameter degeneracy by measuring the T2K off-axis beam in Korea," *Physics Letters B*, vol. 637, no. 4-5, pp. 266–273, 2006.

[96] P. Huber, M. Lindner, and W. Winter, "Synergies between the first-generation JHF-SK and NuMI superbeam experiments," *Nuclear Physics B*, vol. 654, no. 1-2, pp. 3–29, 2003.

[97] H. Minakata, H. Nunokawa, and S. Parke, "Complementarity of eastern and western hemisphere long-baseline neutrino oscillation experiments," *Physical Review D*, vol. 68, no. 1, Article ID 013010, 2003.

[98] V. Barger, D. Marfatia, and K. Whisnant, "How two neutrino superbeam experiments do better than one," *Physics Letters B*, vol. 560, no. 1-2, pp. 75–86, 2003.

[99] K. Whisnant, J. M. Yang, and B.-L. Young, "Measuring CP violation and mass ordering in joint long baseline experiments with superbeams," *Physical Review D*, vol. 67, no. 1, Article ID 013004, 2003.

[100] P. Huber, M. Lindner, M. Rolinec, T. Schwetz, and W. Winter, "Prospects of accelerator and reactor neutrino oscillation experiments for the coming ten years," *Physical Review D*, vol. 70, no. 7, pp. 1–73014, 2004.

[101] O. Mena, "Unveiling neutrino mixing and leptonic CP violation," *Modern Physics Letters A*, vol. 20, no. 1, pp. 1–17, 2005.

[102] O. Mena and S. Parke, "Untangling CP violation and the mass hierarchy in long baseline experiments," *Physical Review D*, vol. 70, no. 9, Article ID 093011, 2004.

[103] T. Akiri, D. Allspach, M. Andrews et al., "The 2010 Interim Report of the Long-Baseline Neutrino Experiment Collaboration Physics Working Groups," In press, http://arxiv.org/abs/1110.6249.

[104] LBNE Reconfiguration, *Steering Committee Interim Report*, June 2012, https://indico.fnal.gov/getFile.py/access?resId=0&materialId=3&confId=5622.

[105] D. Angus, A. Ariga, D. Autiero et al., "The LAGUNA design study-towards giant liquid based underground detectors for neutrino physics and astrophysics and proton decay searches," In press, http://arxiv.org/abs/1001.0077.

[106] A. Rubbia, "A CERN-based high-intensity high-energy proton source for long baseline neutrino oscillation experiments with next-generation large underground detectors for proton decay searches and neutrino physics and astrophysics," In press, http://arxiv.org/abs/1003.1921.

[107] P. Coloma, T. Li, and S. Pascoli, "A comparative study of long-baseline superbeams within LAGUNA for large θ_{13}," In press, http://arxiv.org/abs/1206.4038 .

[108] A. Rubbia, "Underground neutrino detectors for particle and astroparticle Science: the Giant Liquid Argon Charge Imaging ExpeRiment (GLACIER)," *Journal of Physics: Conference Series*, vol. 171, Article ID 012020, 2009.

[109] T. M. Undagoitia, F. V. Feilitzsch, and M. G-Neff, "LENA: a multipurpose detector for low energy neutrino astronomy and proton decay," *Journal of Physics: Conference Series*, vol. 120, Article ID 052018, 2008.

[110] M. Wurm, J. F. Beacom, L. B. Bezrukov et al., "The next-generation liquid-scintillator neutrino observatory LENA," In press, http://arxiv.org/abs/1104.5620.

[111] A. de Bellefon, J. Bouchez, J. Busto et al., "MEMPHYS: a large scale water Cerenkov detector at Frejus," In press, http://arxiv.org/abs/hepex/0607026.

[112] S. K. Agarwalla, T. Li, and A. Rubbia, "An incremental approach to unravel the neutrino mass hierarchy and CP violation with a long-baseline superbeam for large θ_{13}," *Journal of High Energy Physics*, vol. 2012, no. 5, Article ID 154, 2012.

[113] J. Bernabeu, M. Blennow, P. Coloma et al., "EURONU WP6 2009 yearly report: update of the physics potential of Nufact, superbeams and betabeams," Tech. Rep. EURONU-WP6-10-19, 2009.

[114] P. Zucchelli, "A novel concept for a $\overline{\nu}_e/\nu_e$ neutrino factory: the beta-beam," *Physics Letters B*, vol. 532, no. 3-4, pp. 166–172, 2002.

[115] M. Benedikt, A. Bechtold, and F. Borgnolutti, "Conceptual design report for a Beta-Beam facility," *European Physical Journal*, vol. A47, p. 24, 2011.

[116] M. Mezzetto, "Physics reach of the beta beam," *Journal of Physics G*, vol. 29, no. 8, pp. 1771–1776, 2003.

[117] J. Burguet-Castell, D. Casper, J. J. Gómez-Cadenas, P. Hernández, and F. Sánchez, "Neutrino oscillation physics with a higher-$\gamma\beta$-beam," *Nuclear Physics B*, vol. 695, no. 1-2, pp. 217–240, 2004.

[118] J. Burguet-Castell, D. Casper, E. Couce, and J. J. Gómez-Cadenas, "Optimal β-beam at the CERN-SPS," *Nuclear Physics B*, vol. 725, no. 1-2, pp. 306–326, 2005.

[119] A. Donini, E. Fernandez-Martinez, P. Migliozzi et al., "A beta beam complex based on the machine upgrades for the LHC," *European Physical Journal C*, vol. 48, no. 3, pp. 787–796, 2006.

[120] A. Donini and E. Fernández-Martínez, "Alternating ions in a β-beam to solve degeneracies," *Physics Letters B*, vol. 641, no. 6, pp. 432–439, 2006.

[121] A. Donini, E. Fernandez-Martinez, P. Migliozzi et al., "Neutrino hierarchy from CP-blind observables with high density magnetized detectors," *European Physical Journal C*, vol. 53, no. 4, pp. 599–606, 2008.

[122] D. Meloni, O. Mena, C. Orme, S. Palomares-Ruiz, and S. Pascoli, "An intermediate γ beta-beam neutrino experiment with long baseline," *Journal of High Energy Physics*, vol. 2008, no. 7, Article ID 115, 2008.

[123] E. Fernandez-Martinez, "The γ=100 β-Beam revisited," *Nuclear Physics B*, vol. 833, no. 1-2, pp. 96–107, 2010.

[124] C. Orme, "High-Beta Beams within the LAGUNA design study," In press, http://arxiv.org/abs/1004.0939.

[125] P. Coloma, A. Donini, P. Migliozzi, L. Scotto Lavina, and F. Terranova, "A minimal Beta Beam with high-Q ions to address CP violation in the leptonic sector," *European Physical Journal*, vol. C71, p. 1674, 2011.

[126] S. Geer, "Neutrino beams from muon storage rings: characteristics and physics potential," *Physical Review D*, vol. 57, no. 11, pp. 6989–6997, 1998.

[127] A. De Rújula, M. B. Gavela, and P. Hernández, "Neutrino oscillation physics with a neutrino factory," *Nuclear Physics B*, vol. 547, no. 1-2, pp. 21–38, 1999.

[128] A. Bandyopadhyay, S. Choubey, R. Gandhi et al., "Physics at a future neutrino factory and super-beam facility," *Reports on Progress in Physics*, vol. 72, no. 10, Article ID 106201, 2009.

[129] R. J. Abrams, S. K. Agarwalla, A. Alekou et al., "International design study for the neutrino factory, Interim Design Report," In press, http://arxiv.org/abs/1112.2853.

[130] P. Huber and T. Schwetz, "A low energy neutrino factory with non-magnetic detectors," *Physics Letters B*, vol. 669, no. 5, pp. 294–300, 2008.

[131] P. Huber and W. Winter, "Neutrino factories and the "magic" baseline," *Physical Review D*, vol. 68, no. 3, Article ID 037301, 2003.

[132] V. Barger, S. Geer, and K. Whisnant, "Long baseline neutrino physics with a muon storage ring neutrino source," *Physical Review D*, vol. 61, no. 5, Article ID 053004, 2000.

[133] A. Donini, M. B. Gavela, P. Hernández, and S. Rigolin, "Neutrino mixing and CP-violation," *Nuclear Physics B*, vol. 574, no. 1-2, pp. 23–42, 2000.

[134] V. Barger, S. Geer, R. Raja, and K. Whisnant, "Neutrino oscillations at an entry-level neutrino factory and beyond," *Physical Review D*, vol. 62, no. 7, Article ID 073002, pp. 1–12, 2000.

[135] V. Barger, S. Geer, R. Raja, and K. Whisnant, "Long-baseline study of the leading neutrino oscillation at a neutrino factory," *Physical Review D*, vol. 62, no. 1, Article ID 013004, pp. 1–14, 2000.

[136] M. Freund, P. Huber, and M. Lindner, "Systematic exploration of the neutrino factory parameter space including errors and correlations," *Nuclear Physics B*, vol. 615, no. 1—3, pp. 331–357, 2001.

[137] C. Albright, G. Anderson, and V. Barger, "Physics at a neutrino factory," In press, http://arxiv.org/abs/hep-ex/0008064.

[138] M. Apollonio, A. Blondel, and A. Broncano, "Oscillation physics with a neutrino factory," In press, http://arxiv.org/abs/hep-ph/0210192.

[139] P. Huber and W. Winter, "From parameter space constraints to the precision determination of the leptonic Dirac CP phase," *Journal of High Energy Physics*, no. 5, pp. 399–432, 2005.

[140] P. Huber, M. Lindner, M. Rolinec, and W. Winter, "Optimization of a neutrino factory oscillation experiment," *Physical Review D*, vol. 74, no. 7, Article ID 073003, 2006.

[141] A. Donini, P. Huber, S. Pascoli, W. Winter, and O. Yasuda, "Physics and performance evaluation group," in *Proceedings of the 9th International Workshop on Neutrino Factories, Superbeams, and Betabeams (NuFact '07)*, pp. 43–45, August 2007.

[142] S. Geer, O. Mena, and S. Pascoli, "Low energy neutrino factory for large θ_{13}," *Physical Review D*, vol. 75, no. 9, Article ID 093001, 2007.

[143] A. Bross, M. Ellis, S. Geer, O. Mena, and S. Pascoli, "Neutrino factory for both large and small θ_{13}," *Physical Review D*, vol. 77, no. 9, Article ID 093012, 2008.

[144] E. Fernández Martínez, T. Li, S. Pascoli, and O. Mena, "Improvement of the low energy neutrino factory," *Physical Review D*, vol. 81, no. 7, Article ID 073010, 2010.

[145] A. Bueno, M. Campanelli, S. Navas-Concha, and A. Rubbia, "On the energy and baseline optimization to study effects related

to the δ-phase (CP-/T-violation) in neutrino oscillations at a neutrino factory," *Nuclear Physics B*, vol. 631, no. 1-2, pp. 239–284, 2002.

[146] P. Huber and W. Winter, "Neutrino factory superbeam," *Physics Letters B*, vol. 655, no. 5-6, pp. 251–256, 2007.

[147] S. K. Agarwalla, P. Huber, J. Tang, and W. Winter, "Optimization of the neutrino factory, revisited," *Journal of High Energy Physics*, vol. 2011, no. 1, Article ID 120, 2011.

[148] P. Ballett and S. Pascoli, "Understanding the performance of the low-energy neutrino factory: the dependence on baseline distance and stored-muon energy," *Physical Review D*, vol. 86, no. 5, Article ID 053002, 2012.

[149] P. Coloma, P. Huber, J. Kopp, and W. Winter, "Systematic uncertainties in long-baseline neutrino oscillations for large θ_{13}," In press, http://arxiv.org/abs/1209.5973.

[150] D. Indumathi and N. Sinha, "Effect of tau neutrino contribution to muon signals at neutrino factories," *Physical Review D*, vol. 80, no. 11, Article ID 113012, 2009.

[151] A. Donini, J. J. Gómez Cadenas, and D. Meloni, "The τ-contamination of the golden muon sample at the Neutrino Factory," *Journal of High Energy Physics*, vol. 2011, no. 2, Article ID 095, 2011.

[152] P. Huber, "On the determination of anti-neutrino spectra from nuclear reactors," *Physical Review D*, vol. C84, no. 2, Article ID 024617, 16 pages, 2011.